Journal of Quantitative Spectroscopy & Radiative Transfer 109 (2008) 2219–2243

Journal of Quantitative Spectroscopy & Radiative Transfer

www.elsevier.com/locate/jqsrt

Ground-based solar absorption studies for the Carbon Cycle science by Fourier Transform Spectroscopy (CC-FTS) mission

Dejian Fu[a], Keeyoon Sung[a], Chris D. Boone[a], Kaley A. Walker[a,b], Peter F. Bernath[a,c,*]

[a]*Department of Chemistry, University of Waterloo, Waterloo, ON, Canada N2L 3G1*
[b]*Department of Physics, University of Toronto, Toronto, ON, Canada M5S 1A7*
[c]*Department of Chemistry, University of York, York, YO10 5DD, UK*

Received 11 June 2007; received in revised form 11 February 2008; accepted 12 February 2008

Abstract

Carbon cycle science by Fourier transform spectroscopy (CC-FTS) is an advanced study for a future satellite mission. The goal of the mission is to obtain a better understanding of the carbon cycle in the Earth's atmosphere by monitoring total and partial columns of CO_2, CH_4, N_2O, and CO in the near infrared. CO_2, CH_4, and N_2O are important greenhouse gases, and CO is produced by incomplete combustion. The molecular O_2 column is also needed to obtain the effective optical path of the reflected sunlight and is used to normalize the column densities of the other gases. As part of this advanced study, ground-based Fourier transform spectra are used to evaluate the spectral region and resolution needed. Spectra in the 3950–7140 cm^{-1} region with a spectral resolution of 0.0042 cm^{-1} recorded at Kiruna (67.84°N, 20.41°E, and 419 m above sea level), Sweden, on 1 April 1998, were degraded to the resolutions of 0.01, 0.1, and 0.3 cm^{-1}. The effect of spectral resolution on the retrievals has been investigated with these four Kiruna spectra. To obtain further information on the spectral resolution, optical components and spectroscopic parameters required by the future mission, high-resolution solar absorption spectra between 2000 and 15000 cm^{-1} were recorded using Fourier transform spectrometers at Kitt Peak (31.9°N, 111.6°W, and 2.1 km above sea level), Arizona, on 25 July 2005 and Waterloo (43.5°N, 80.6°W, and 0.3 km above sea level), Ontario, on 22 November 2006 with spectral resolutions of 0.01 and 0.1 cm^{-1}, respectively. Dry air volume mixing ratios (VMRs) of CO_2 and CH_4 were retrieved from these ground-based observations. The HITRAN 2004 spectroscopic parameters are used with the SFIT2 package for the spectral analysis. The measurement precisions for CO_2 and CH_4 total columns are better than 1.07% and 1.13%, respectively, for our observations. Based on these results, a Fourier transform spectrometer (maximum spectral resolution of 0.1 cm^{-1} or 5 cm maximum optical path difference (MOPD)) operating between 2000 and 15000 cm^{-1} is suggested as the primary instrument for the mission. Further progress in improving the atmospheric retrievals for CO_2, CH_4, and O_2 requires new laboratory measurements of the spectroscopic line parameters.

Keywords: Carbon cycle; Atmospheric absorption spectra; Fourier transform spectroscopy; HITRAN 2004; O_2 A band; Carbon dioxide; Methane; Nitrous oxide; Carbon monoxide; Averaging kernels; SFIT2

*Corresponding author at: Department of Chemistry, University of Waterloo, Waterloo, ON, Canada N2L 3G1. Fax: +44 1904 432516.
E-mail address: pfb500@york.ac.uk (P.F. Bernath).

0022-4073/$ - see front matter
doi:10.1016/j.jqsrt.2008.02.003

1. Introduction

Emissions from human activities such as combustion of fossil fuel, production of cement, and changes in land use are changing the Earth's atmosphere. The primary anthropogenic contribution to the change in atmospheric composition is the emission of the greenhouse gases CO_2, CH_4, and N_2O [1–4]. Greenhouse gas concentrations in the atmosphere have increased significantly in the past few decades [2–9]. The first high-precision measurements of atmospheric CO_2 concentrations on a continuous basis were taken by Keeling starting in 1958 at Mauna Loa, Hawaii [6,10]. The record of CO_2 concentrations at Mauna Loa, now known as the "Keeling curve", indicates a 21% increase in the mean annual concentration from 315 ppmv in 1958 to 381 ppmv in 2006 as shown in Fig. 1. (Source data are available at ftp://ftp.cmdl.noaa.gov/ccg/co2/in-situ/.) The persistent year-to-year increase has an associated wave-like pattern in each year. These annual cycles are due to the effect of the biosphere on the CO_2 concentration. The atmospheric CO_2 concentration is higher in winter due to biospheric respiration and has low values in summer because of drawdown by photosynthesis [5,6]. The increase in greenhouse gases has important consequences for air quality, meteorology, and climate [1–4,11].

Since the 1970s, a world-wide network of more than 100 stations has been organized to monitor greenhouse gases. For example, air samples are collected through the National Ocean and Atmospheric Administration (NOAA)/Earth System Research Laboratory global network, including a cooperative program for carbon-containing gases which provides samples from 30 fixed stations and at 5° latitude intervals from three ship routes [2,3]. In North America, solar absorption spectra recorded containing information on CH_4 and CO_2 have been recorded since 1978 at Kitt Peak, in Arizona [7–9]. The tropospheric CH_4 and atmospheric CO_2 total columns were retrieved from these spectra. In 1992, the Kyoto Protocol was established as an international treaty on climate change, assigning mandatory greenhouse gas emission limitations to the signatory countries [3,11].

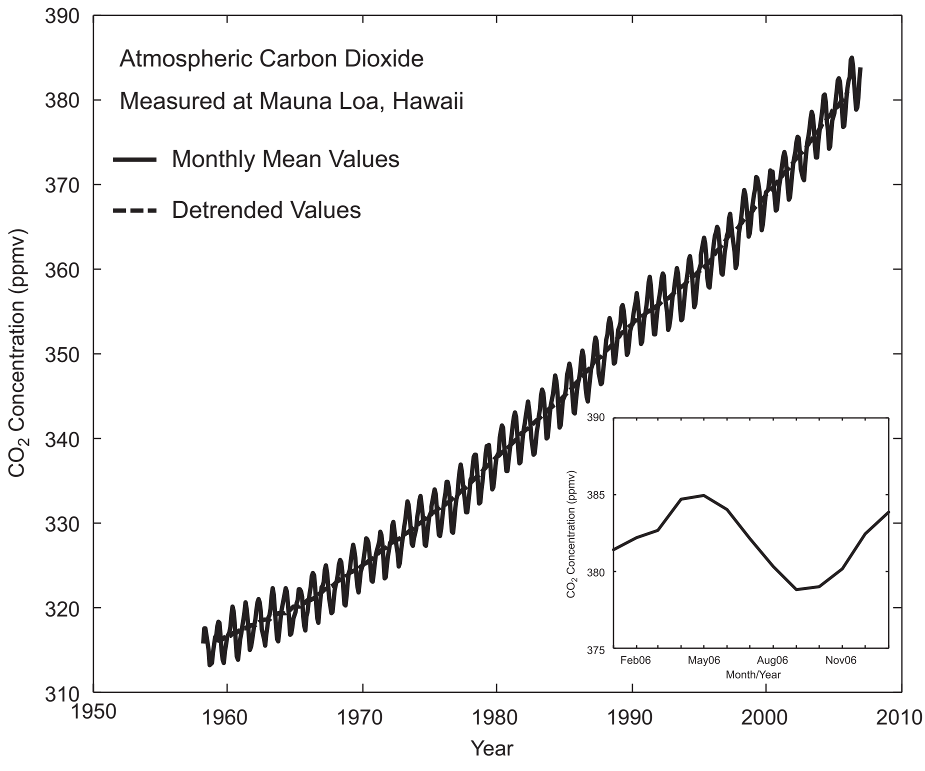

Fig. 1. The 48-year record of atmospheric CO_2 monthly mean concentrations in dry air at Mauna Loa, also known as the Keeling curve, shows a 21% increase of the mean annual concentration from 315 ppmv in 1958 to 381 ppmv in 2006. The annual cycle of CO_2 at Mauna Loa in 2006 is shown in the subplot. Source data were obtained from the following link: ftp://ftp.cmdl.noaa.gov/ccg/co2/in-situ/.

Detailed knowledge of the carbon cycle is necessary to implement the Kyoto Protocol and successor agreements. Measurements from ground-based instruments provide long-term records of concentrations of major greenhouse gases but with limited spatial coverage. Furthermore, in the transport models used to identify the regional sources and sinks, errors within models are bigger than those between models [12]. The requirement to improve our knowledge of sources and sinks of greenhouse gases makes the knowledge of the global spatial distributions important and, for example, precise global space-based CO_2 observations can improve carbon flux inversions as illustrated by several sensitivity studies [13–18]. Observations from space using Fourier transform spectroscopy (FTS) provide an effective method to obtain global distributions of greenhouse gases with high spatial resolution and accuracy. Current satellite instruments such as TOVS [19,20], AIRS [20,21], IASI [20,22], TES [23], MOPITT [24,25], and particularly SCIAMACHY [26,27] are carrying out pioneering studies on global carbon budgets. However, measurements from these missions have a limitation in that they provide a precision not better than 1% for the columns and, except for SCIAMACHY, all of them have poor sampling of the planetary boundary layer [28]. Since differential column distributions are needed to identify regional sources and sinks of CO_2, it is the precision of the measurements that is more important than absolute accuracy. In 1997, Park showed that a precision of better than 1% in the CO_2 column-averaged volume mixing ratio (VMR) can be achieved for a FTS when the O_2 A-band and three CO_2 bands at 4.3, 2.7, and 2.0 μm are employed [29]. Recent studies by Rayner et al. in 2001 [13] demonstrated that a precision of 2.5 ppm (0.7%) is needed to improve on the current knowledge of sources and sinks based on the existing flask network. The absolute accuracy can be improved by a ground-based, calibration–validation program associated with a satellite mission.

The Orbiting Carbon Observatory (OCO) mission will make the first global, space-based measurements of atmospheric carbon dioxide (CO_2) with the precision, resolution, and coverage required to characterize CO_2 sources and sinks on regional scales. Starting in 2008, the OCO mission will measure global CO_2 column densities using three nadir-viewing near-infrared grating spectrometers (spectral resolution of about $0.3\,\mathrm{cm}^{-1}$) in a 98.2° polar sun-synchronous orbit in the 'A-train' [28]. The Greenhouse Gases Observing Satellite (GOSAT) mission will also be launched in 2008 and will use a Fourier transform spectrometer (resolution of $0.2\,\mathrm{cm}^{-1}$, maximum optical path difference (MOPD) = 2.5 cm) to make measurements of additional gases such as CH_4 as well as CO_2 [30]. GOSAT will use nadir observations in the thermal infrared as well as the near infrared, but has a measurement pixel size of 10 by 10 km [30] compared to 1 by 1 km used by OCO [28]. Smaller pixel sizes suffer from less cloud contamination. SCIAMACHY on Envisat is currently making remarkable near-infrared observations of CO_2, CH_4, and CO total columns at moderate spectral resolution [31–33]. The lack of a targeted glint mode, however, means SCIAMACHY rarely provides useful data over water and the large pixel size (26 by 15 km), means that most pixels are cloud-contaminated [32]. The carbon cycle science by FTS (CC-FTS) mission is a second generation mission proposed to follow OCO and GOSAT. It aims to provide highly precise simultaneous observations of CO_2, CH_4, CO, N_2O, and O_2 with a small pixel size of 1 by 1 km similar to the OCO mission.

This paper reports on the results of ground-based observations needed to select the spectral regions, spectral resolution, and spectroscopic line parameter requirements for this proposed mission. In previous studies, solar absorption spectra recorded in the near infrared have been analyzed to obtain CH_4 and CO_2 columns [7–9]. However, the spectroscopic parameters from HITRAN 1996 and 2000 used in their work are substantially different from more recent values [34–36]. In the near infrared, nadir satellite observations are based on the measurement of reflected sunlight [37–41]. Solar photons experience significant scattering in the atmosphere from clouds and aerosols and therefore have an effective optical path different from that calculated using the observation geometry. The retrieved column densities of the greenhouse gases can be corrected for the variations in optical path caused by clouds and aerosols by dividing them by the simultaneously observed O_2 total column. O_2 is a well-mixed gas with a known constant VMR. However, no published work has used spectra of the O_2 A-band at 0.76 μm and the greenhouse gas absorptions in the near-infrared region (such as CH_4 near 1.68 μm and CO_2 near 1.57 and 2.06 μm) which were simultaneously observed from ground. Most of the ground-based FTSs such as those used in the Network for the Detection of Atmospheric Composition Change only observe in the infrared from 700 to $7000\,\mathrm{cm}^{-1}$ [http://www.ndsc.ncep.noaa.gov/]. Recently, automated observatories with the capability of measuring atmospheric column abundances of CO_2 and O_2 simultaneously using near-infrared FTS spectra of the sun have been developed in the Total Carbon Column

Observing Network. The first observations at Park Fall, Wisconsin, have just been published, but they did not use the O_2 A-band measurements in their analyses [42]. Simultaneously observed spectra are able to provide the total column of CO_2, CH_4, CO, N_2O, and O_2 at the same atmospheric conditions such as optical path and ambient pressure. Our work presents first results from ground-based measurements over a broad spectral region spanning 2000–15,000 cm^{-1}.

2. Instrumentation and observations

The effect of spectral resolution has been considered in order to determine an optimum value for a greenhouse gas mission. Ground-based atmospheric absorption spectra in the 3950–7140 cm^{-1} region with a spectral resolution of 0.0042 cm^{-1} (120 cm MOPD) recorded using a Bruker IFS 120 HR spectrometer at Kiruna (67.84°N, 20.41°E, and 419 m above sea level), Sweden, on 1 April 1998 [43] were used for this study. The observed interferogram was truncated at 50, 5, and 5/3 cm optical path difference and Fourier transformed to generate spectra with resolution of 0.01, 0.1, and 0.3 cm^{-1}, respectively. Figs. 2–5 present expanded views of observed and resolution-degraded spectra in six spectral regions including CO_2 at 4911 and 6238 cm^{-1}, CH_4 at 4264 and 5891 cm^{-1}, CO at 4274 cm^{-1}, and N_2O at 4429 cm^{-1}. Typical molecular line widths due to pressure broadening are 0.1 cm^{-1} in the troposphere, so there is little change in the spectra as the resolution changes from 0.0042 to 0.01 cm^{-1} and even to 0.1 cm^{-1} for these molecules. The change in resolution from 0.1 to 0.3 cm^{-1}, however, has a more significant effect and in all cases, except for the very clean CO_2 band near 6239 cm^{-1} that has been selected as the primary candidate for CO_2 column measurements, there is a serious loss of information at the lowest spectral resolution of 0.3 cm^{-1} for the atmospheric species of CH_4, CO, and N_2O. In particular, the lines of interest become blended with water lines and the baseline is no longer clear; this will degrade the retrieval precision. To monitor concentrations of major greenhouse species other than CO_2 with high precision, the spectral resolution should be higher than 0.3 cm^{-1}. Spectra recorded at about 0.1 cm^{-1} (MOPD = 5 cm) are satisfactory.

For additional studies, we recorded atmospheric absorption spectra with resolutions of 0.01 and 0.1 cm^{-1} at the National Solar Observatory (NSO) at Kitt Peak in Arizona (31.9°N, 111.6°W, and 2.1 km above sea level) and the Waterloo Atmospheric Observatory (WAO) at Waterloo in Ontario (43.5°N, 80.6°W, and 0.3 km above sea level). A series of spectra were obtained on 25 July 2005 using the McMath–Pierce Fourier transform spectrometer, a folded cat's-eye Michelson interferometer (MOPD = 100 cm) housed in a vacuum vessel in the McMath–Pierce solar telescope facility at the NSO. An ABB Bomem DA8 Fourier transform spectrometer, a plane mirror Michelson interferometer (25 cm MOPD), was used for the observations at the WAO on 22 November 2006.

For the observations at NSO, an indium antimonide (InSb) detector and calcium fluoride (CaF_2) beamsplitter were used to record atmospheric absorption spectra from 2000 to 15,000 cm^{-1}. Each spectrum recorded is the coaddition of two scans (about 30 min) at a spectral resolution of 0.01 cm^{-1}. A RG715 filter was used to cut the spectra at 15,000 cm^{-1}. At WAO, the observations were also recorded in the near-infrared spectral region from 2000 to 15,000 cm^{-1}, in order to obtain spectroscopic signatures of O_2, CH_4, CO_2, CO, and N_2O. A filter (713 nm or 14,000 cm^{-1} red pass) in front of the entrance window of the DA8 spectrometer was used to block visible light. InSb and semiconductor silicon (Si) detectors were used (InSb: 2000–15,000 cm^{-1}, Si: 8500–15,000 cm^{-1}) in alternation. Each spectrum is obtained from the coaddition of 20 scans (about 15 min).

The upper plot in Fig. 6 shows an overview of the atmospheric absorption spectra recorded at WAO covering the broad spectral region from mid-infrared to visible. The spectral segments indicated by the solid bars are the regions containing a high density of absorption features of CH_4, CO_2, CO, N_2O, and O_2. The lower plot in Fig. 6 provides enlarged views of three spectral regions of interest. Starting from the top, they are CO_2 at 1.58 μm, CO_2 at 2.06 μm, and O_2 at 0.76 μm recorded with the InSb detector. The bottom plot shows O_2 at 0.76 μm recorded using the Si detector. The O_2 A-band recorded using the InSb detector has a signal-to-noise ratio (SNR) of 150:1. Although the InSb detector is not optimal for the 0.76 μm spectral region, spectra recorded with the InSb detector are similar in quality as those acquired using the Si detector. The highest precision results will be obtained by using spectra covering all regions of interest (including the A-band) that are recorded at the same time [7–9,42]. Hence, our analysis only includes spectra recorded using the InSb detector.

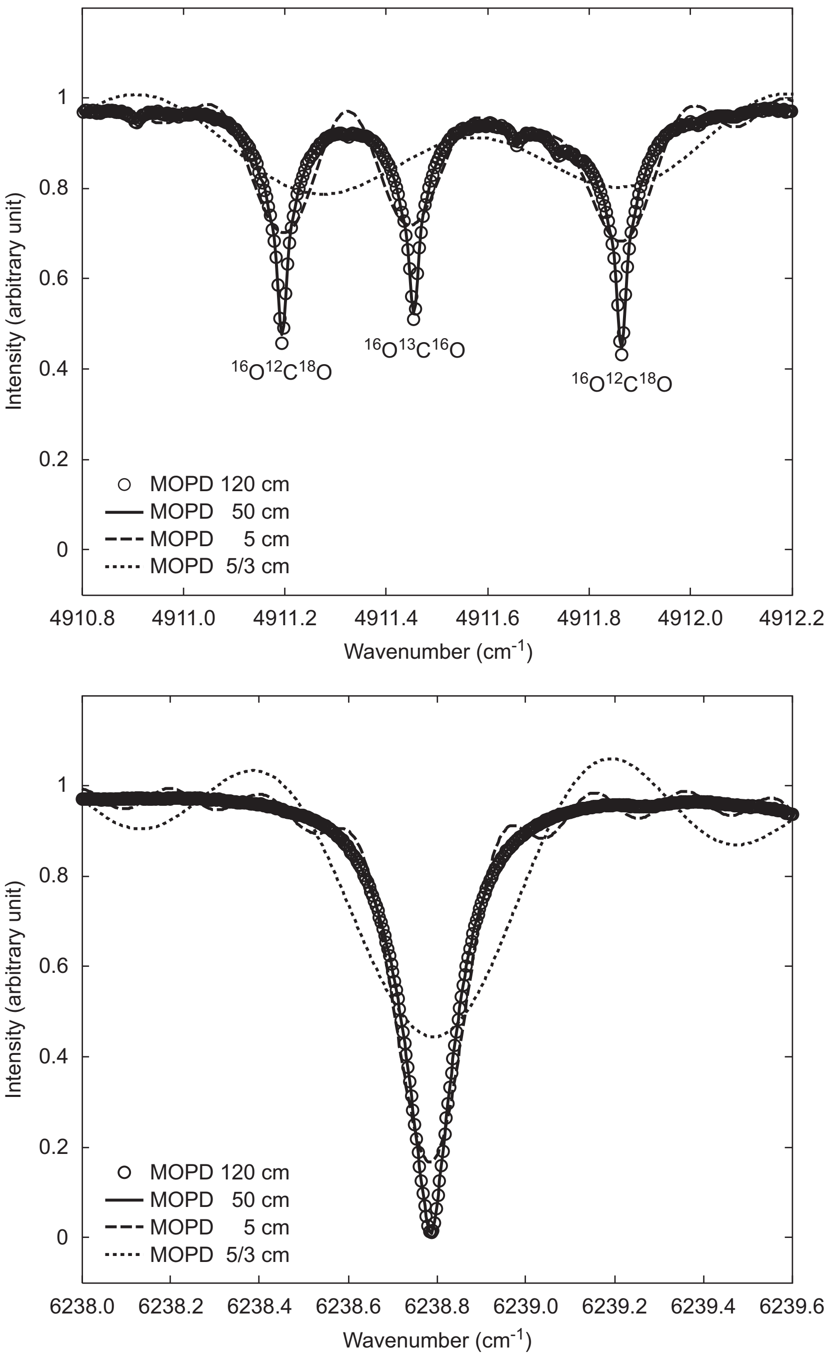

Fig. 2. Observed and resolution-degraded atmospheric absorption spectra of CO_2 near 4911 cm^{-1} (2.06 μm) (upper plot) and near 6238 cm^{-1}(1.57 μm) (lower plot) are shown. Circles indicate spectra recorded with a Bruker IFS 120 HR spectrometer by Meier at IRF Kiruna (67.84°N, 20.41°E, and 419 m above sea level) on 1 April 1998. Solar zenith angle is 65.02°, and the spectral resolution is 0.0042 cm^{-1} (MOPD = 120 cm). Spectra with resolution degraded from 0.0042 (MOPD = 120 cm) to 0.01 cm^{-1} (MOPD = 50 cm), 0.1 (MOPD = 5 cm), and 0.3 cm^{-1} (MOPD = 5/3 cm) are presented by circles, solid line, dashed line, and dotted line, respectively.

3. Spectral analysis and retrievals

Spectra recorded at the two observatories were analyzed using SFIT2 (version 3.91) [44,45]. SFIT2 is widely used for the analysis of ground-based solar absorption spectra and was jointly developed at the NASA-Langley

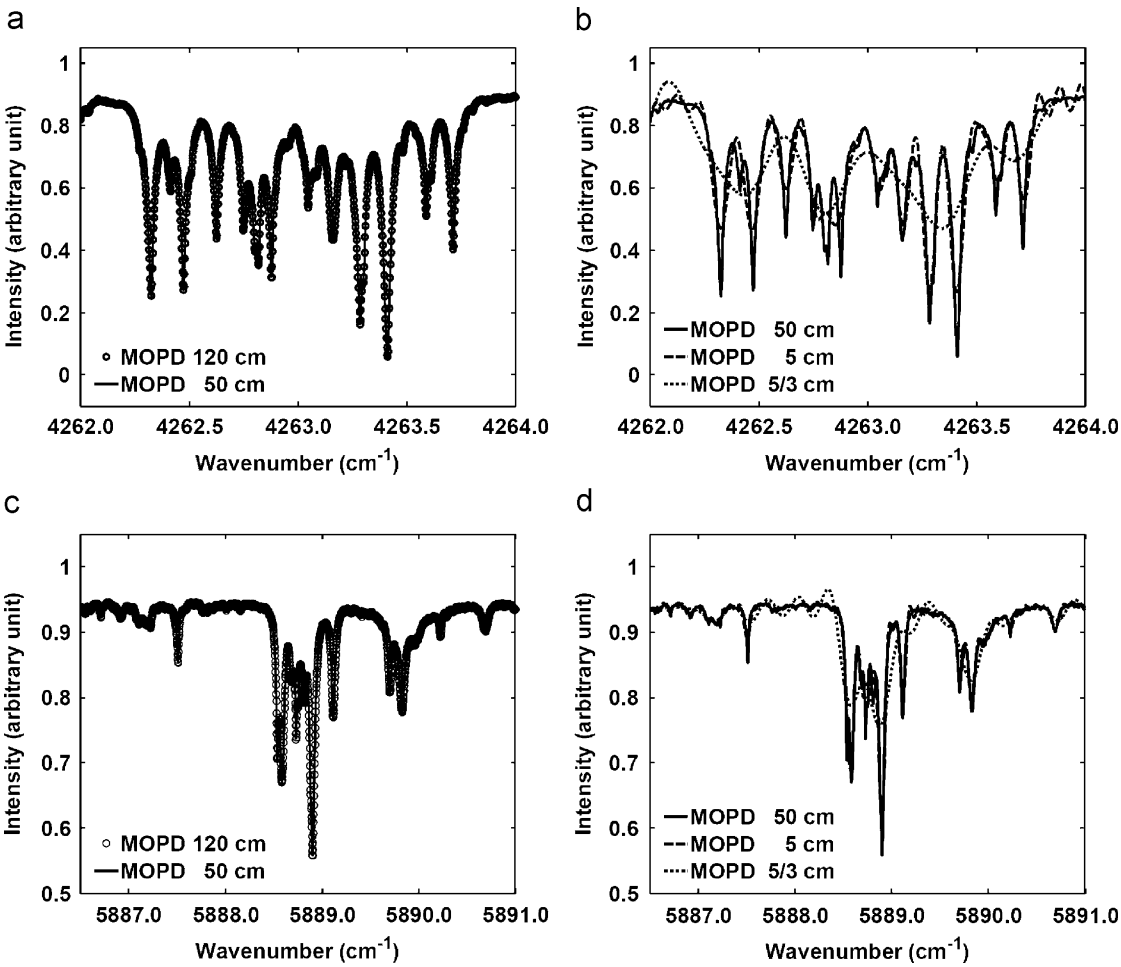

Fig. 3. Observed and resolution-degraded atmospheric absorption spectra of CH_4 near 4263 cm^{-1} (2.34 μm) (plots a–b) and near 5889 cm^{-1} (1.69 μm) (plots c–d) are shown. Circles indicate spectra recorded with a Bruker IFS 120 HR spectrometer by Meier at IRF Kiruna (67.84°N, 20.41°E, and 419 m above sea level) on 1 April 1998. Solar zenith angle is 65.02°, and spectral resolution is 0.0042 cm^{-1} (MOPD = 120 cm). Spectra with resolution degraded from 0.0042 to 0.01 cm^{-1} (MOPD = 50 cm), 0.1 (MOPD = 5 cm), and 0.3 cm^{-1} (MOPD = 5/3 cm) are shown by circles, solid line, dashed line, and dotted line, respectively.

Research Center and at the National Institute of Water and Atmospheric Research at Lauder, New Zealand. SFIT2 is a retrieval algorithm that employs the Optimal Estimation Method (OEM) of Rodgers et al. [46–49]. It makes use of the OEM to include *a priori* constituent profiles as a function of altitude in the retrievals in a statistically sound manner. SFIT2 allows the simultaneous retrieval of a vertical profile and column density of the target molecule together with the total columns of interfering species.

Model atmospheres are used in the SFIT2 program to simulate spectra during the retrievals. A program called FSCATM [50] was used to carry out refractive ray tracing needed to generate the model atmospheres using *a priori* state estimates, pressure profiles, and temperature profiles. The *a priori* VMR profiles used in the retrievals of spectra recorded at WAO were generated by Wiacek [51,52]. A combination of a climatology estimated from the HALogen Occultation Experiment version 19 solar sunset occultation profiles [53] within $\pm 5°$ in latitude and longitude of the Toronto Atmospheric Observatory which is an observatory about 90 km away from WAO, mid-latitude daytime 2001 Michelson Interferometer for Passive Atmospheric Sounding reference profiles [54], and the Jet Propulsion Laboratory (JPL) MkIV FTS balloon flight data [55] were used to construct the *a priori* state estimates of VMR profiles and columns. The *a priori* VMRs from the observations of the JPL MkIV balloon Fourier transform infrared spectra obtained in northern mid-latitudes

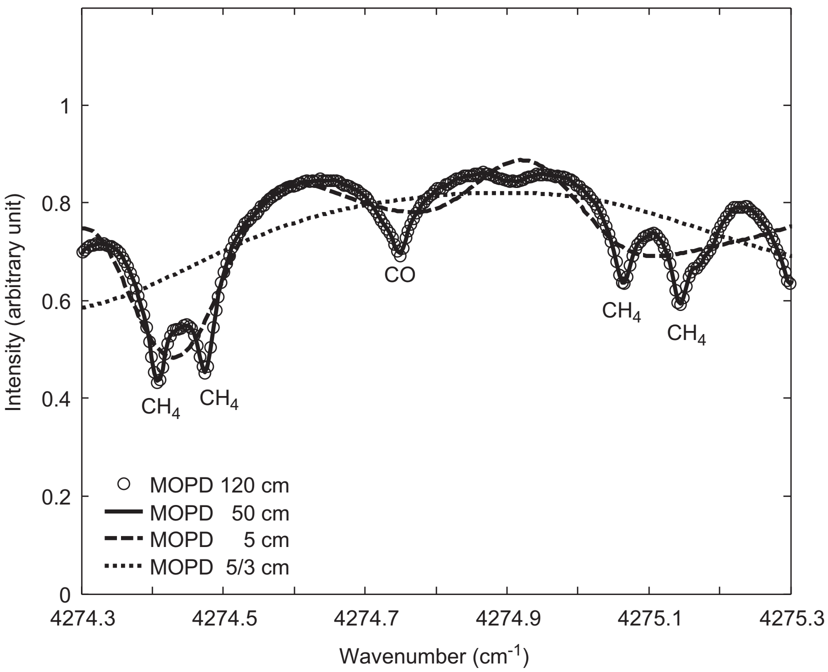

Fig. 4. Observed and resolution-degraded atmospheric absorption spectra of CO near 4274 cm^{-1} (2.34 μm) are shown. Circles indicate spectra recorded with a Bruker IFS 120 HR spectrometer by Meier at IRF Kiruna (67.84°N, 20.41°E, and 419 m above sea level) on 1 April 1998. Solar zenith angle is 65.02°, and the spectral resolution is 0.0042 cm^{-1} (MOPD = 120 cm). Spectra with resolution degraded from 0.0042 to 0.01 cm^{-1} (MOPD = 50 cm), 0.1 cm^{-1} (MOPD = 5 cm), and 0.3 cm^{-1} (MOPD = 5/3 cm) are presented by circles, solid line, dashed line, and dotted line, respectively.

by Toon et al. [55], Stratospheric Processes And their Role in Climate 2000 (SPARC2000) [56], and the Atmospheric Chemistry Experiment Fourier Transform Spectrometer [57,58] are used in the retrievals of Kitt Peak spectra. Two sets of *a priori* estimates are used in retrievals because there are significant environmental differences between the two sites. The impact of *a priori* has been investigated by carrying out the retrievals of spectra recorded at Waterloo using *a priori* for Kitt Peak. We found that the impacts are fairly small in the averaging kernels for our observations. Pressure and temperature profiles for the retrievals of spectra recorded at WAO and NSO were obtained from the National Centers for Environmental Prediction (NCEP)/National Center for Atmospheric Research analyses provided by the NASA Goddard Space Flight Centre automailer (obtained from the Goddard Automailer science@hyperion.gsfc.nasa.gov) [59,60] and the Mass-Spectrometer-Incoherent-Scatter model (MSIS-2000) [61]. NCEP covers the surface to 50 km and the output of MSIS is used from 50 to 100 km. The spectroscopic line parameters used in this work are from the High resolution TRANsmission molecular absorption database (HITRAN) 2004 [62].

In our analysis, we mainly focus on CO_2 and CH_4, two greenhouse gases that are identified in the Intergovernmental Panel on Climate Change 2007 report as the first and second most important species in altering the balance of incoming and outgoing energy in the Earth-atmosphere system [4]. Total columns of CO_2 were retrieved from three spectral bands: two bands at 1.57 μm and one band at 2.06 μm. The absorption features at 1.57 μm consist of 30013–00001 ($v_1+4v_2+v_3$, $v_0 = 6228\,cm^{-1}$) and 30012–00001 ($2v_1+2v_2+v_3$, $v_0 = 6348\,cm^{-1}$) transitions. They will be referred to as the CO_2 6228 and CO_2 6348 cm^{-1} bands. In the spectral region at 1.57 μm, there are numerous absorption features from CO_2 with weak absorption by H_2O, HDO, and additionally CH_4 for the 30013–00001 transition. These bands consist of many lines with a wide range of intensities, which provides good retrieval sensitivities in both the stratosphere and troposphere. Thermal emission from the atmosphere and instrument is also negligible at these short wavelengths [63]. The 2.06 μm CO_2 absorption band has a weaker dependence on the CO_2 concentration and greater sensitivity to airborne particles and the temperature profile than the weaker absorption in the 1.57 μm bands [16].

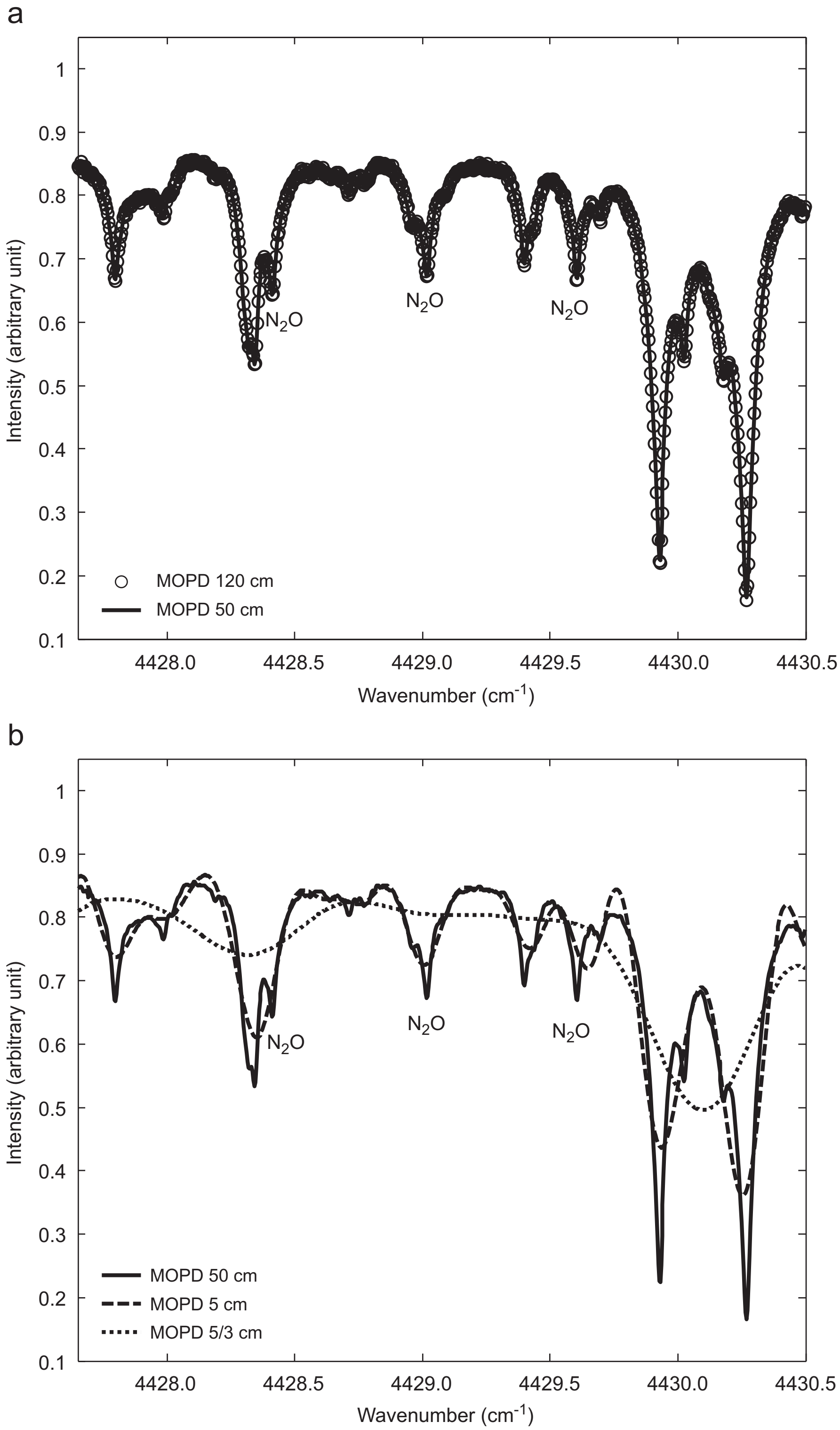

Fig. 5. Observed and resolution-degraded atmospheric absorption spectra of N_2O near 4429 cm^{-1} (2.26 μm) (plots a–b) are shown. Circles indicate spectra recorded with a Bruker IFS 120 HR spectrometer by Meier at IRF Kiruna (67.84°N, 20.41°E, and 419 m above sea level) on 1 April 1998. Solar zenith angle is 65.02°, and spectral resolution is 0.0042 cm^{-1} (MOPD = 120 cm). Spectra with resolution degraded from 0.0042 to 0.01 cm^{-1} (MOPD = 50 cm), 0.1 (MOPD = 5 cm), and 0.3 cm^{-1} (MOPD = 5/3 cm) are presented by circles, solid line, dashed line, and dotted line, respectively.

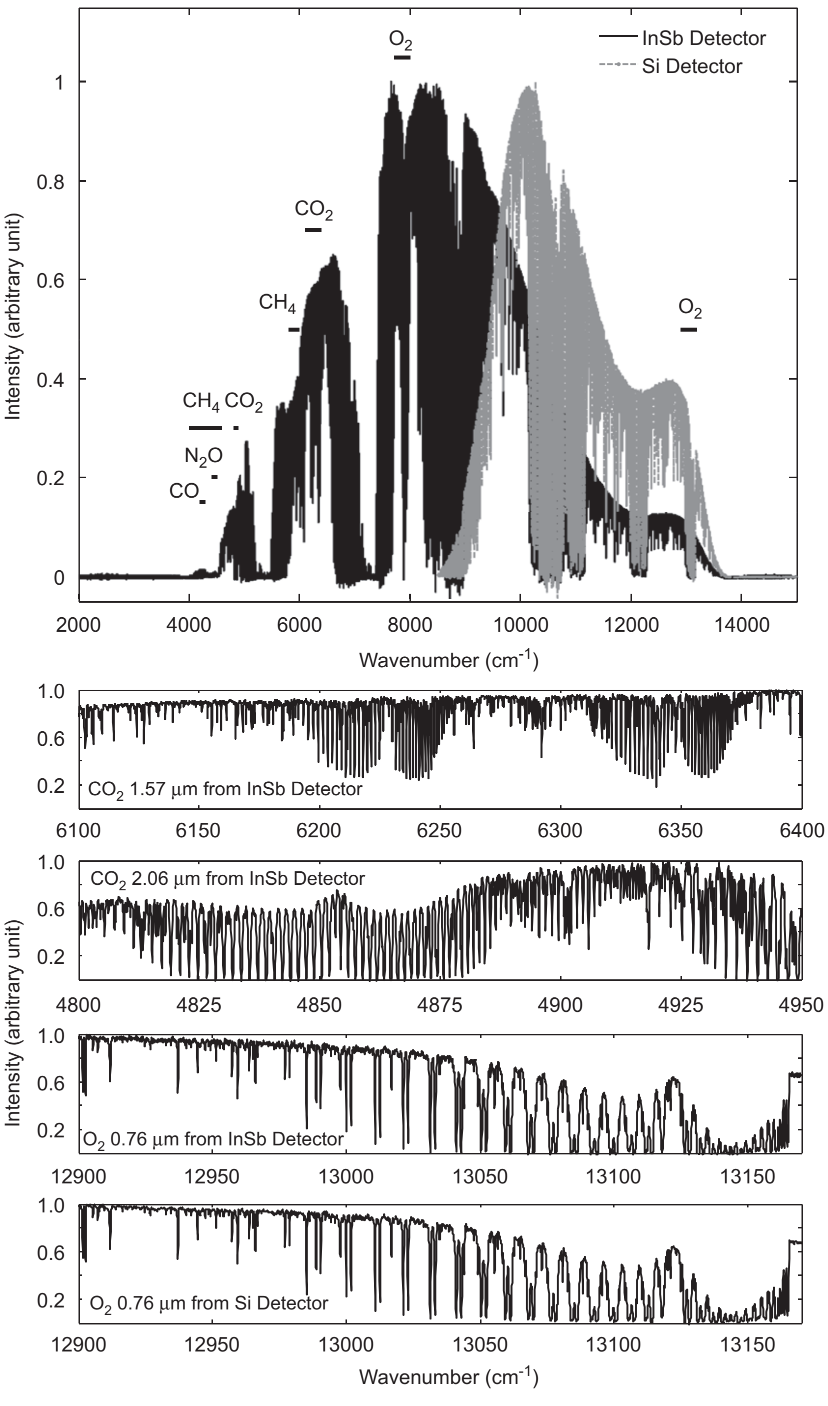

Fig. 6. Overview (upper plot) and enlarged view (lower plot) of the atmospheric absorption spectra recorded on 22 November 2006, using an ABB Bomem DA8 spectrometer at Waterloo Atmospheric Observatory (WAO) (43.5°N, 80.6°W, and 0.3 km above sea level) are shown. Spectral resolution is 0.1 cm^{-1} (MOPD = 5 cm). InSb and Si detectors are used to record spectra covering the spectral region from 4000 to 14,000 cm^{-1} (solid line in upper plot) and 8500 to 14,000 cm^{-1} (dash line in upper plot), respectively. Solar zenith angles are 66.61° and 67.33° for InSb and Si data, respectively. In the overview of spectra, solid bars with species names indicate the spectral regions containing suitable absorption features. From top to bottom in the right plot, expanded spectral sections from the overview spectra are shown for CO_2 at 1.57 and 2.06 μm, O_2 A-band at 0.76 μm from InSb and Si detectors, respectively.

The spectral region from 5880 to 5996 cm^{-1} was investigated for the CH_4 retrieval, taking advantage of its weak dependence on the temperature profile [8]. The total column of O_2 will be used to overcome the common systematic bias in CH_4 and CO_2 retrievals arising from air mass errors and surface pressure variations. Spectra of the O_2 A-band at 0.76 μm provide constraints on both the surface pressure and optical path length variations associated with scattering by aerosols in the atmosphere [37–41]. By taking the ratio of columns of CH_4 and CO_2 to O_2 columns, systematic errors will be reduced as long as they are measured under the same conditions. The O_2 total columns were retrieved from the ${}^1\Delta_g - {}^3\Sigma_g^-$ IR band ($\nu_0 = 7882\,cm^{-1}$) at 1.27 μm and the $b^1\Sigma_g^+ - X^3\Sigma_g^-$ band ($\nu_0 = 13121\,cm^{-1}$) (A-band) at 0.76 μm. Two sets of line intensity parameters for the O_2 7882 cm^{-1} band are used based on the work of Goldman (private communication) and the values in HITRAN 2004 [62].

4. Results and discussion

Figs. 7–12 show sample fits for CO_2, CH_4, and O_2 using spectra recorded at NSO and WAO. The largest discrepancies between the calculated and the measured transmittances are on the order of a few percent and are observed in the vicinity of the absorption line centers. Similar systematic fitting residual patterns in terms of positions and amplitudes also appeared in the results of previous work [7–9,41]. They mainly arise from the spectroscopic parameters including line intensity, self- and air-broadening coefficients, and self- and air-shift coefficients. Away from the absorption lines, the fitting residuals from spectra recorded at NSO are generally larger than those obtained using spectra recorded at WAO. This is because the WAO spectra have a higher SNR mainly because of their lower spectral resolution.

The absolute accuracy of the CO_2 retrievals obtained using spectroscopic parameters from HITRAN 2004 is expected to be limited to ~2% [64]. Recent studies show the improvements in the CO_2 spectroscopic parameters in the spectral region of 4550–7000 cm^{-1}, with a precision of 1% or better [35,36,64–67]. Very recently, Devi et al. [64] made further improvements in the CO_2 spectroscopic parameters for the 6348 cm^{-1} band by considering line mixing and using speed-dependent Voigt line shape functions. This work by Devi et al. provides the possibility of remote sensing CO_2 with ~0.3% precision. As demonstrated by Boone et al. [68], the use of speed-dependent Voigt line shape functions improves tropospheric remote sensing, but such a modification of SFIT2 is beyond the scope of this paper. Deficiencies in spectroscopic parameters were also found for the CH_4 and O_2 retrievals. For example, the fitting residuals show obvious difficulty in fitting the O_2 continuum (not included in our forward model) for both 1.27 and 0.76 μm bands. However, no recent published work has presented improvements to the spectroscopic parameters for CH_4 and O_2 over those in HITRAN 2004.

Sources and sinks for greenhouse gases are located primarily in the boundary layer. Hence it is critical for any satellite mission to obtain good sensitivity near the surface. The vertical sampling of a particular measurement is quantified by computing the averaging kernel as defined in the Rodgers optimal estimation approach [48]. The Rodgers approach for a retrieval such as the vertical profile of CO_2 combines information from observations and the *a priori* values in a statistically sound manner. The averaging kernel is the derivative of a derived parameter with respect to its *a priori* state value, i.e., when this derivative is small (nearly 0) all of the information comes from *a priori* data, and when it is large (near 1) the information in the retrieval comes mainly from the measured data. When observing the atmosphere with a nadir viewing geometry, a spectrometer with higher spectral resolution is expected to provide better vertical information than one with low spectral resolution. Typical vertical averaging kernels for CO_2 at 2.06 and 1.57 μm, CH_4 at 1.68 μm from ground-based observations at NSO and WAO are shown in Figs. 9 and 13–15. They demonstrate that our observations achieved the required near-surface sensitivity, i.e., averaging kernel values are near one from the surface to the upper troposphere. In this altitude range, only minor differences are seen between spectra with resolutions of 0.01 and 0.1 cm^{-1}. The retrieval of a tropospheric partial column at a spectral resolution of 0.1 cm^{-1} is as feasible as that for a spectrum with 0.01 cm^{-1} resolution. For CO_2 observations at NSO and WAO, the full width at half maximum (FWHM) of the averaging kernel profiles has similar values (about 10 km) for the two spectral resolutions for the layer from the surface to 8 km and the layer from 8 to 15 km. For the case of CH_4, the FWHM of the averaging kernel profiles is also similar for the two spectral resolutions and is about 12 km for the layer from the surface to 8 km and for the layer from 8 to 15 km.

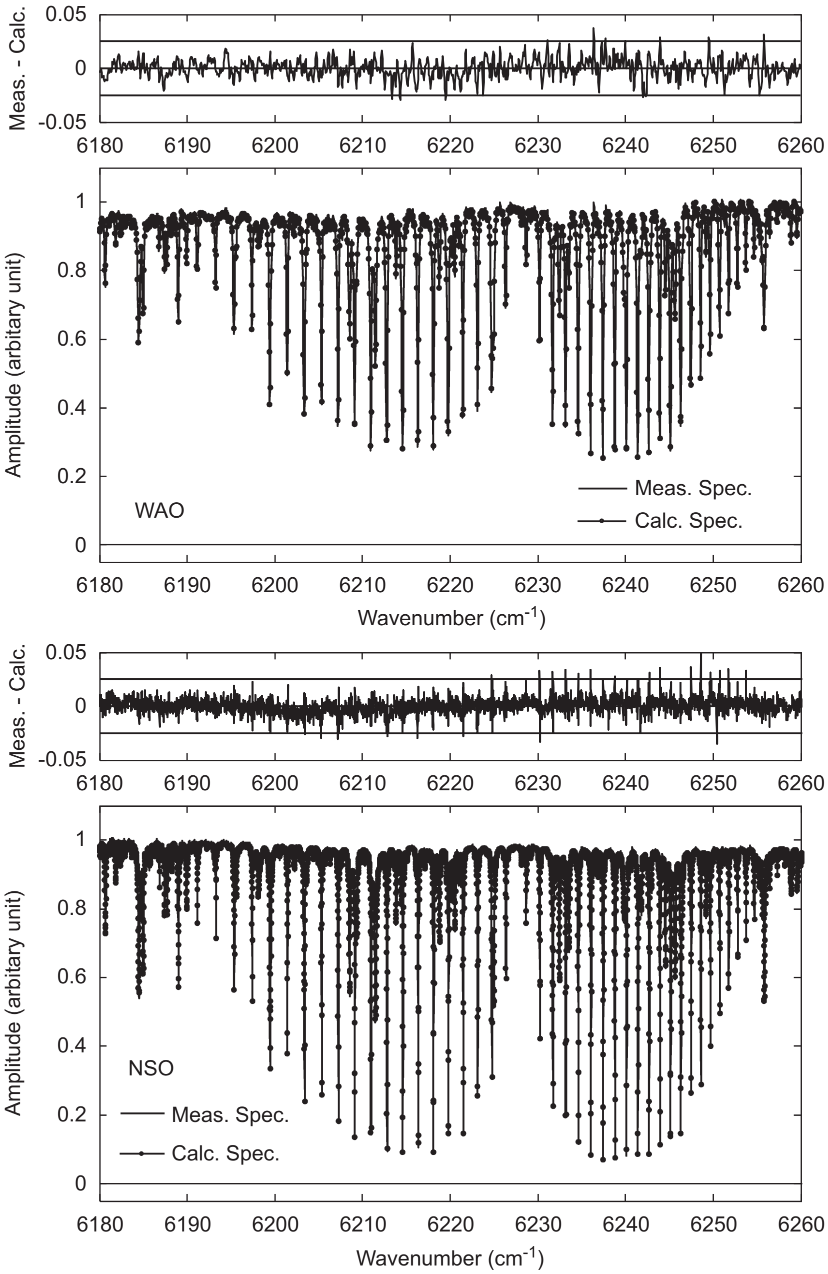

Fig. 7. Fitting residuals for CO_2 6228 cm^{-1} band (6180–6260 cm^{-1}) at 1.57 μm obtained using spectra recorded at WAO on 22 November 2006 (spectral resolution: 0.1 cm^{-1}, solar zenith angle: 66.6°) and obtained using spectra recorded at National Solar Observatory (NSO) (31.9°N, 111.6°W, and 2.1 km above sea level) at Kitt Peak in Arizona on 25 July 2005 (spectral resolution: 0.01 cm^{-1}, solar zenith angle: 49.1°) are shown in the upper and lower plots, respectively.

There is enough information to split the total CO_2 column and the CH_4 column into four layers and two layers, respectively. A FTS with lower spectral resolution (0.1 cm^{-1}) will provide spectra with a higher SNR, and is much cheaper to build than one with a higher resolution (0.01 cm^{-1}).

The previous study of Mao and Kawa in 2004 [17] also suggests that a spectral resolution of about 0.1 cm^{-1} is sufficient for the observation of greenhouse gases from space. They demonstrate that a spectral resolution of 0.07 cm^{-1} near 1.58 μm is suitable for observing of CO_2 in the planetary boundary layer. In addition,

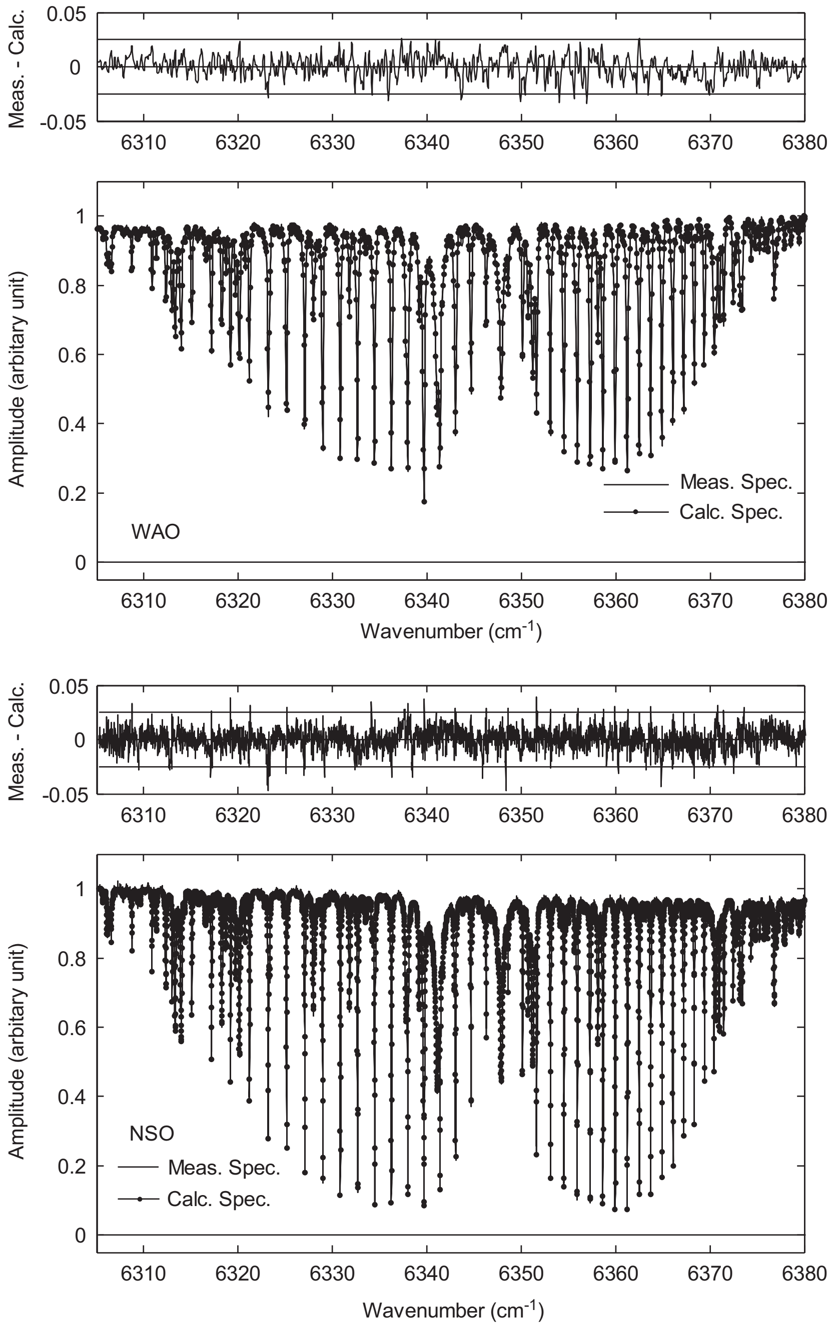

Fig. 8. Fitting residuals for CO_2 6348 cm^{-1} band at 1.57 μm (6305–6380 cm^{-1}) obtained using spectra recorded at WAO on 22 November 2006 (spectral resolution: 0.1 cm^{-1}, solar zenith angle: 66.6°) and obtained using spectra recorded at NSO on 25 July 2005 (spectral resolution: 0.01 cm^{-1}, solar zenith angle: 49.1°) are shown in the upper and lower plots, respectively.

Bösch et al. in 2006 [32] and Barkley et al. 2007 [69] evaluated the sensitivity of SCIAMACHY retrievals of CO_2 from the surface to 20 km. The averaging kernel values for SCIAMACHY drop rapidly with altitude to a value of 0.2 at 20 km, i.e., only about 20% of information is from the observations as shown in Fig. 3 of Bösch et al. in 2006 [32] and Fig. 2 of Barkely et al. in 2007 [69]. In contrast, the averaging kernels for the observations carried out in this work show much better sensitivity (Figs. 9 and 13–15) than those of SCIAMACHY due to the higher spectral resolution of the FTS data obtained at WAO and NSO.

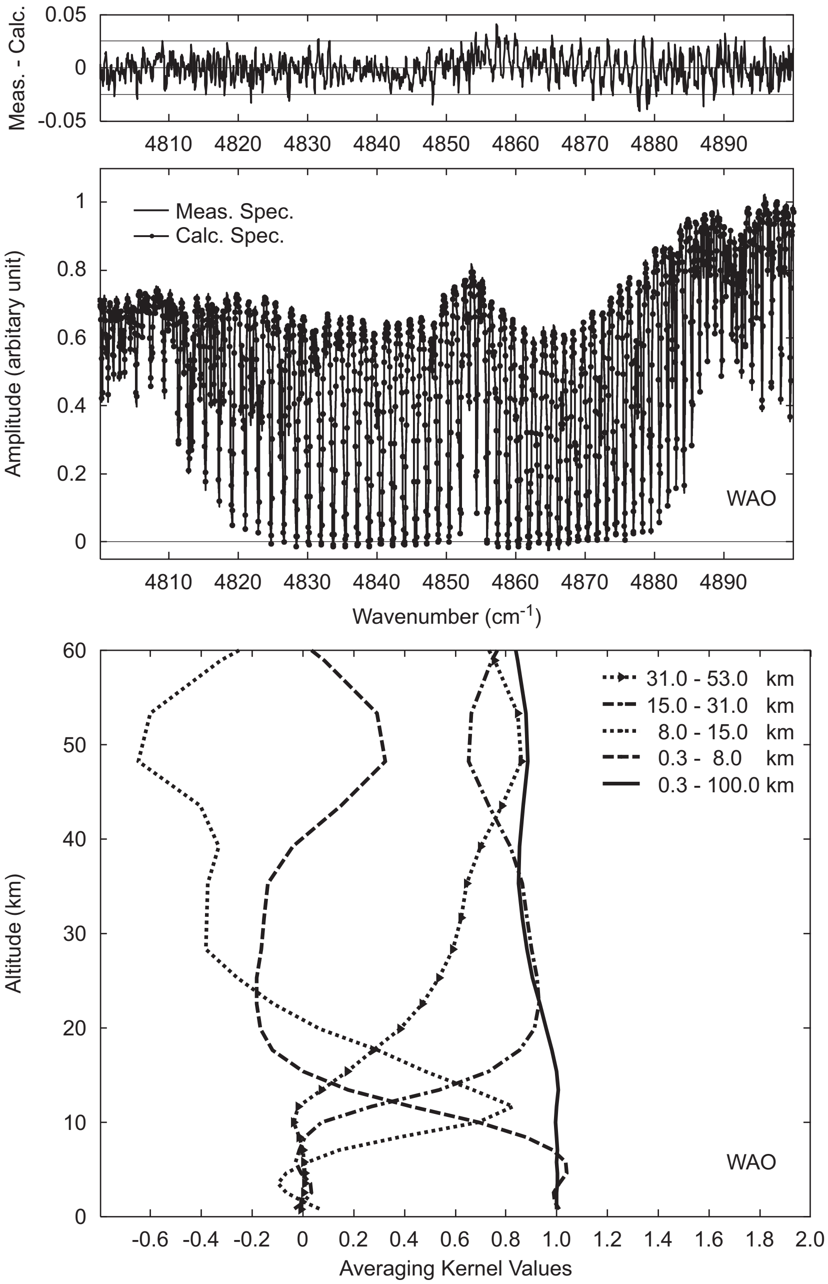

Fig. 9. Fitting residuals for CO_2 at 2.06 μm (4800–6900 cm^{-1}) obtained using spectra recorded at WAO on 22 November 2006 (spectral resolution: 0.1 cm^{-1}, solar zenith angle: 66.6°) and averaging kernel profiles corresponding to the retrievals are shown in the upper and lower plots, respectively.

The retrievals using the SFIT2 program provide the total vertical column density of CO_2, and the column-averaged VMR of CO_2 can be calculated using

$$\mathrm{VMR}_{CO_2} = \frac{C_{CO_2}}{C_{air}} \tag{1}$$

However, the VMRs have only limited precision because the measurements are influenced by a number of factors such as variations in surface pressure and light path in the atmosphere. Humidity can increase the total

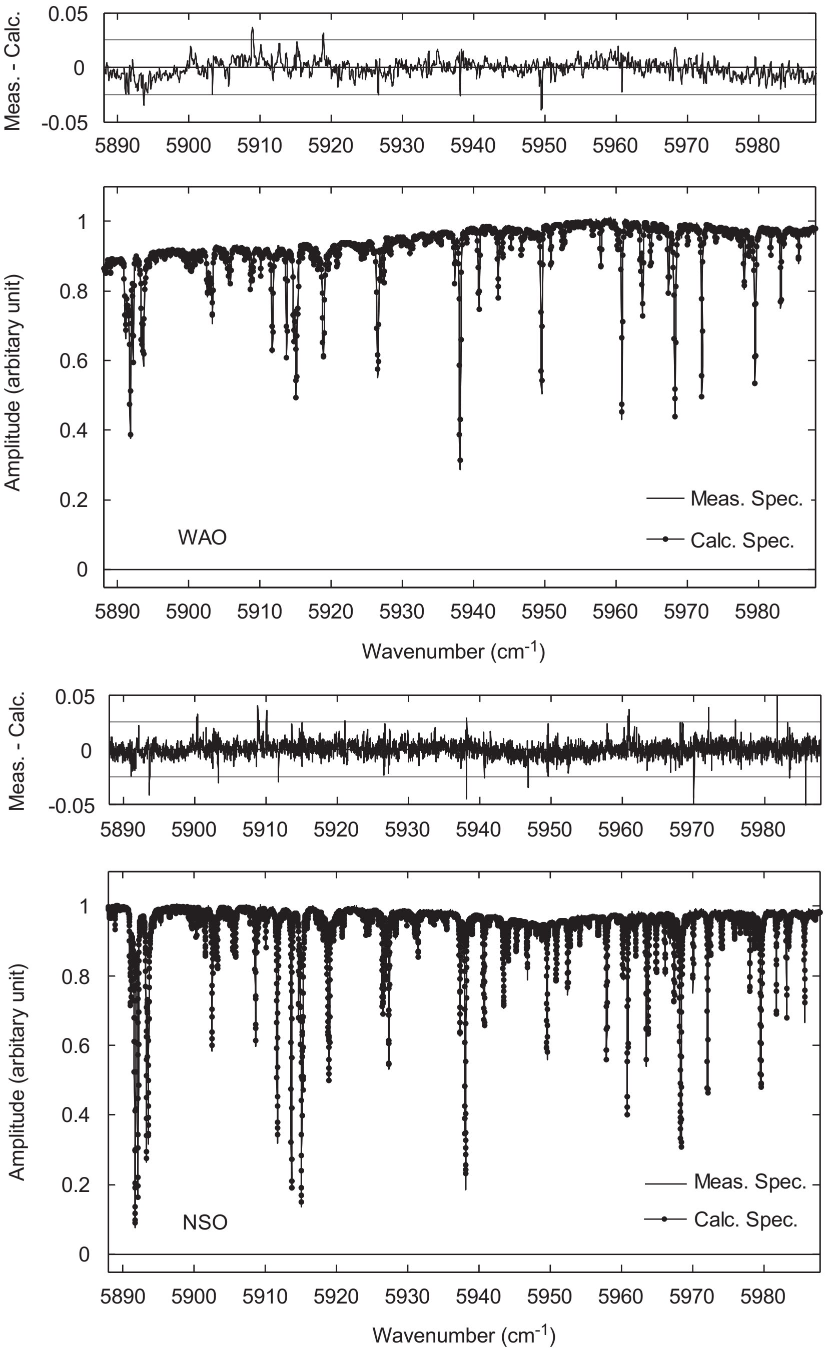

Fig. 10. Fitting residuals for CH_4 at 1.68 μm (5888–5990 cm^{-1}) obtained using spectra recorded at WAO on 22 November 2006 (spectral resolution: 0.1 cm^{-1}, solar zenith angle: 66.6°) and obtained using spectra recorded at NSO on 25 July 2005 (spectral resolution: 0.01 cm^{-1}, solar zenith angle: 49.1°) are shown in the upper and lower plots, respectively.

column of air by 0.5%, but does not change the CO_2 total column. Essentially the CO_2 gets 'diluted' by the H_2O. Fortunately, the O_2 total vertical column density is diluted in the same way as CO_2 and has a similar optical path. The VMR of CO_2 in dry air is more directly related to sources and sinks and is a better tracer because it is not influenced by evaporation or condensation of H_2O. The VMR of O_2 in dry air can be assumed

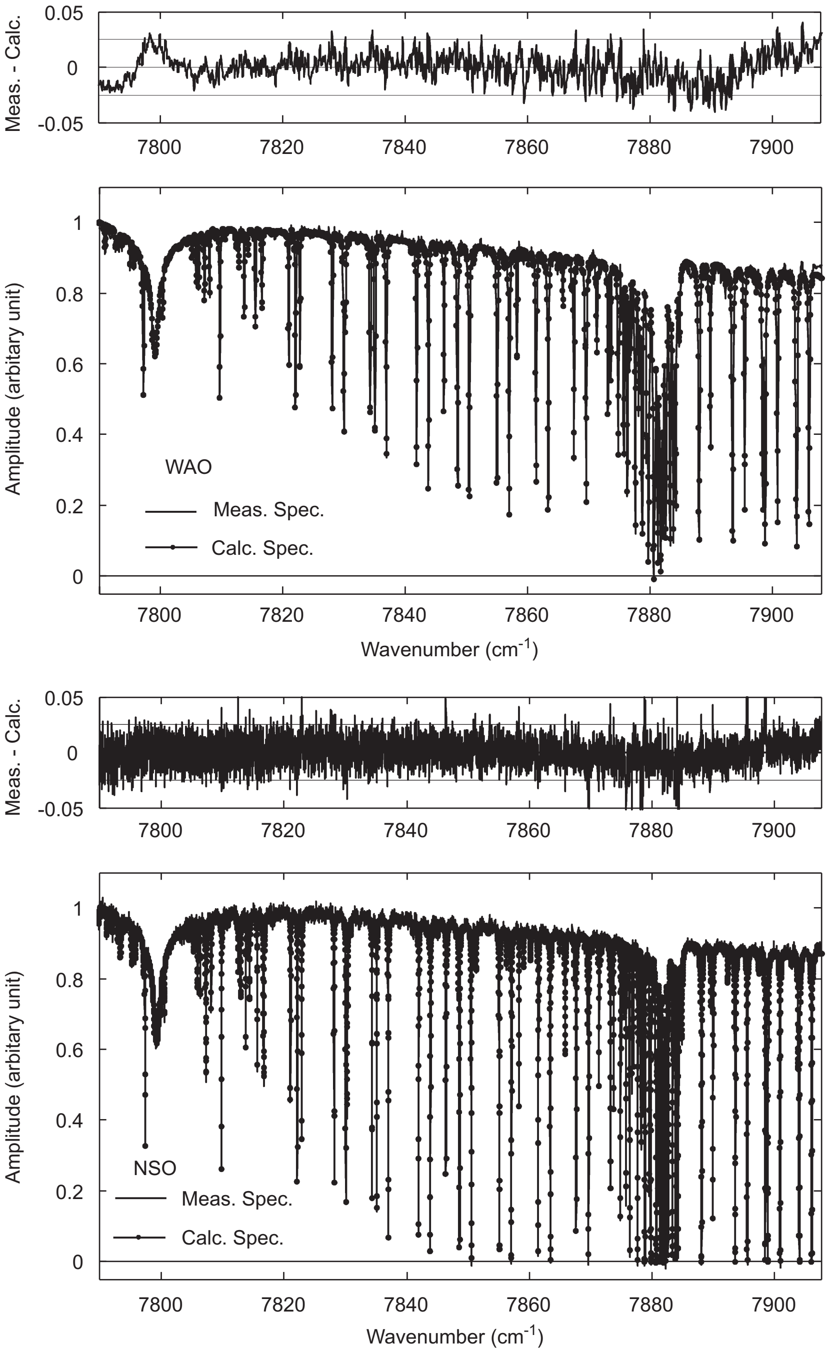

Fig. 11. Fitting residuals for O_2 at 1.27 μm (7790–7908 cm^{-1}) obtained using spectra recorded at WAO on 22 November 2006 (spectral resolution: 0.1 cm^{-1}, solar zenith angle: 66.6°) and obtained using spectra recorded at NSO on 25 July 2005 (spectral resolution: 0.01 cm^{-1}, solar zenith angle: 49.1°) are shown in the upper and lower plots, respectively.

to be constant at 0.2095, so the total column of dry air is given by

$$C_{\text{dry-air}} = \frac{C_{O_2}}{0.2095} \tag{2}$$

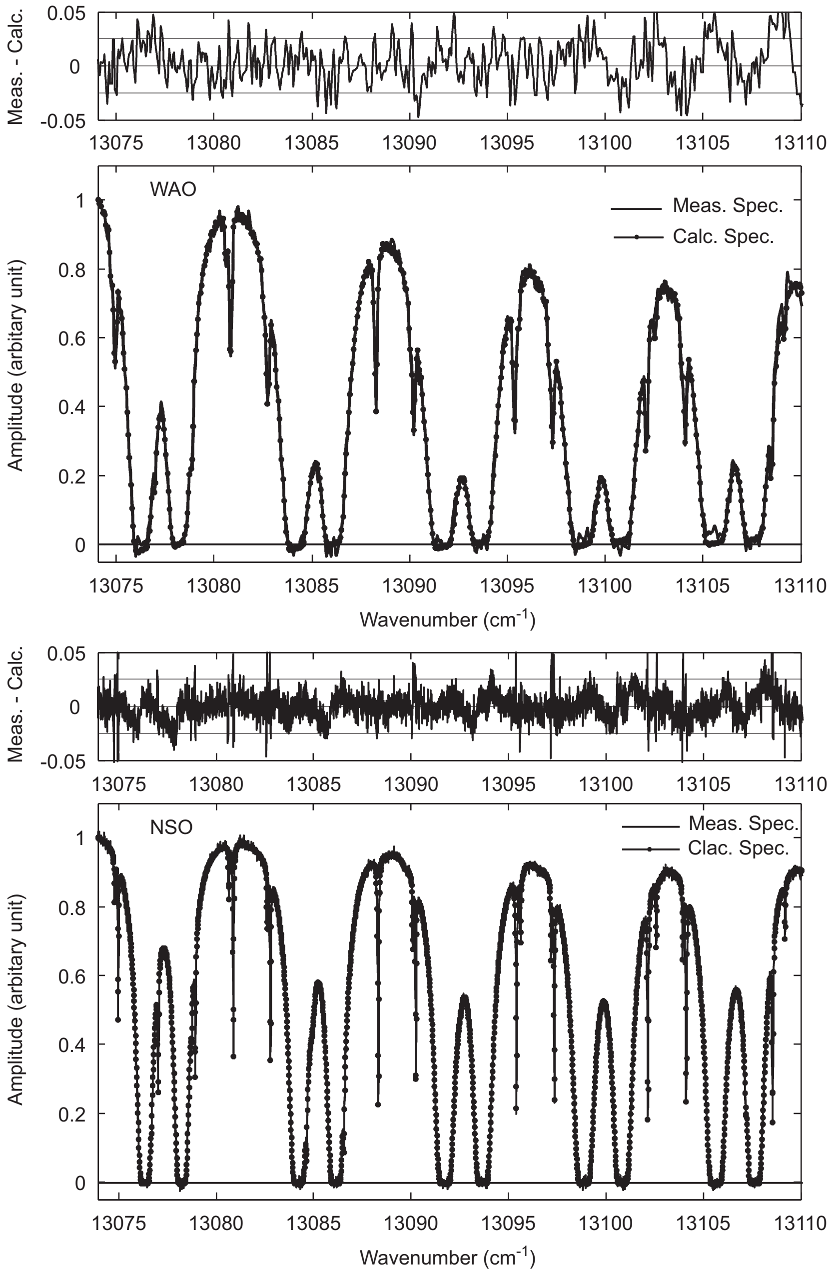

Fig. 12. Fitting residuals for O_2 A-band at 0.76 μm (13,074–13,110 cm^{-1}) obtained using spectra recorded at WAO on 22 November 2006 (spectral resolution: 0.1 cm^{-1}, solar zenith angle: 66.6°) and obtained using spectra recorded at NSO on 25 July 2005 (spectral resolution: 0.01 cm^{-1}, solar zenith angle: 49.1°) are shown in the upper and lower plots, respectively.

The retrieved O_2 total vertical column density obtained from the O_2 A-band is used in Eq. (2). By replacing the total vertical column density of air in Eq. (1) with the total columns of dry air obtained from Eq. (2), the VMR of CO_2 in dry air is

$$\mathrm{VMR}_{\mathrm{dry}\text{-}\mathrm{CO_2}} = \frac{0.2095 \times C_{\mathrm{CO_2}}}{C_{\mathrm{O_2}}} \tag{3}$$

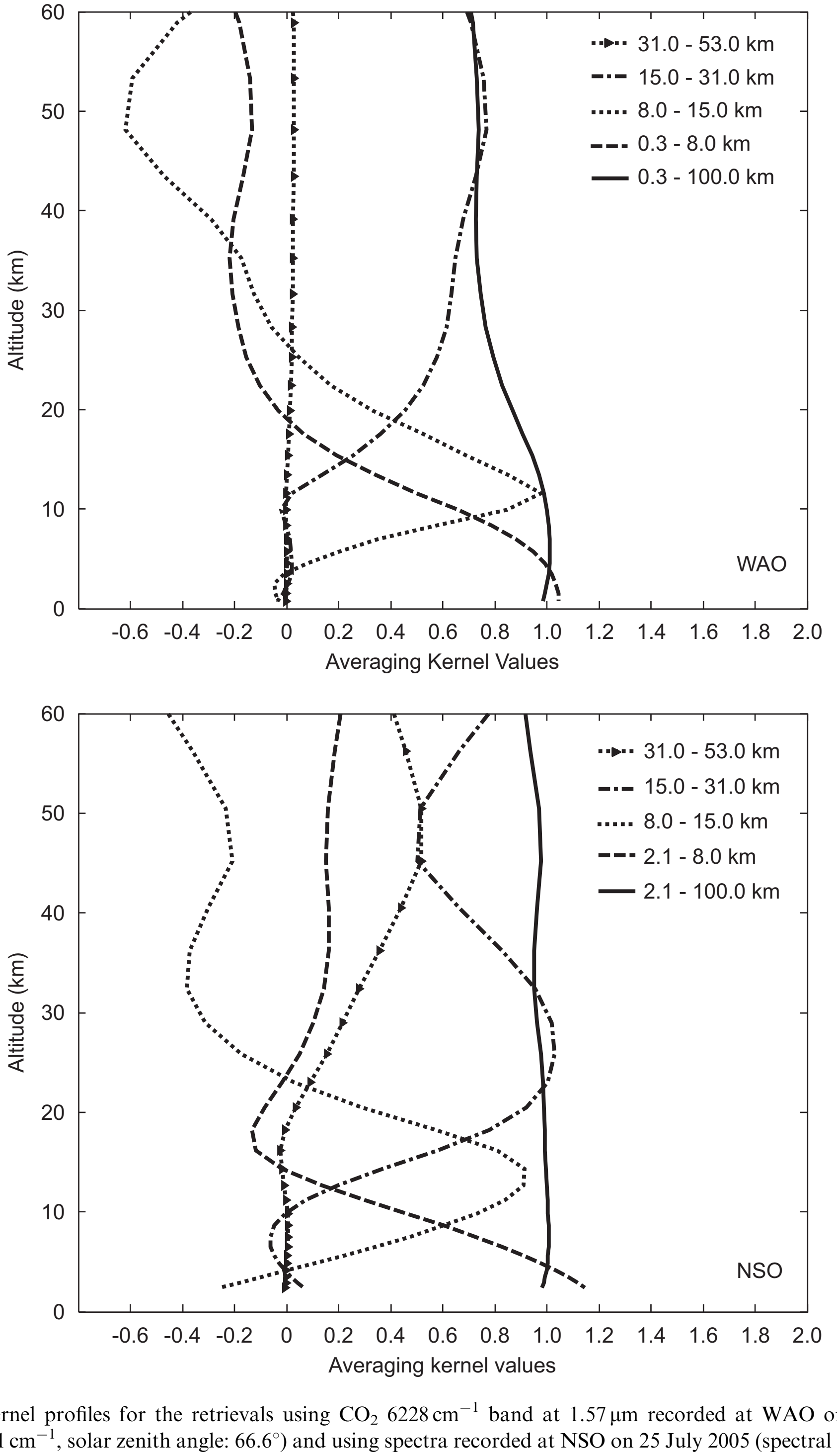

Fig. 13. Averaging kernel profiles for the retrievals using CO_2 6228 cm^{-1} band at 1.57 μm recorded at WAO on 22 November 2006 (spectral resolution: 0.1 cm^{-1}, solar zenith angle: 66.6°) and using spectra recorded at NSO on 25 July 2005 (spectral resolution: 0.01 cm^{-1}, solar zenith angle: 49.1°) are shown in the upper and lower plots, respectively.

Eq. (3) can be adapted to give the CH_4 VMR in dry air as

$$\mathrm{VMR}_{\mathrm{dry}\text{-}\mathrm{CH_4}} = \frac{0.2095 \times C_{\mathrm{CH_4}}}{C_{\mathrm{O_2}}} \tag{4}$$

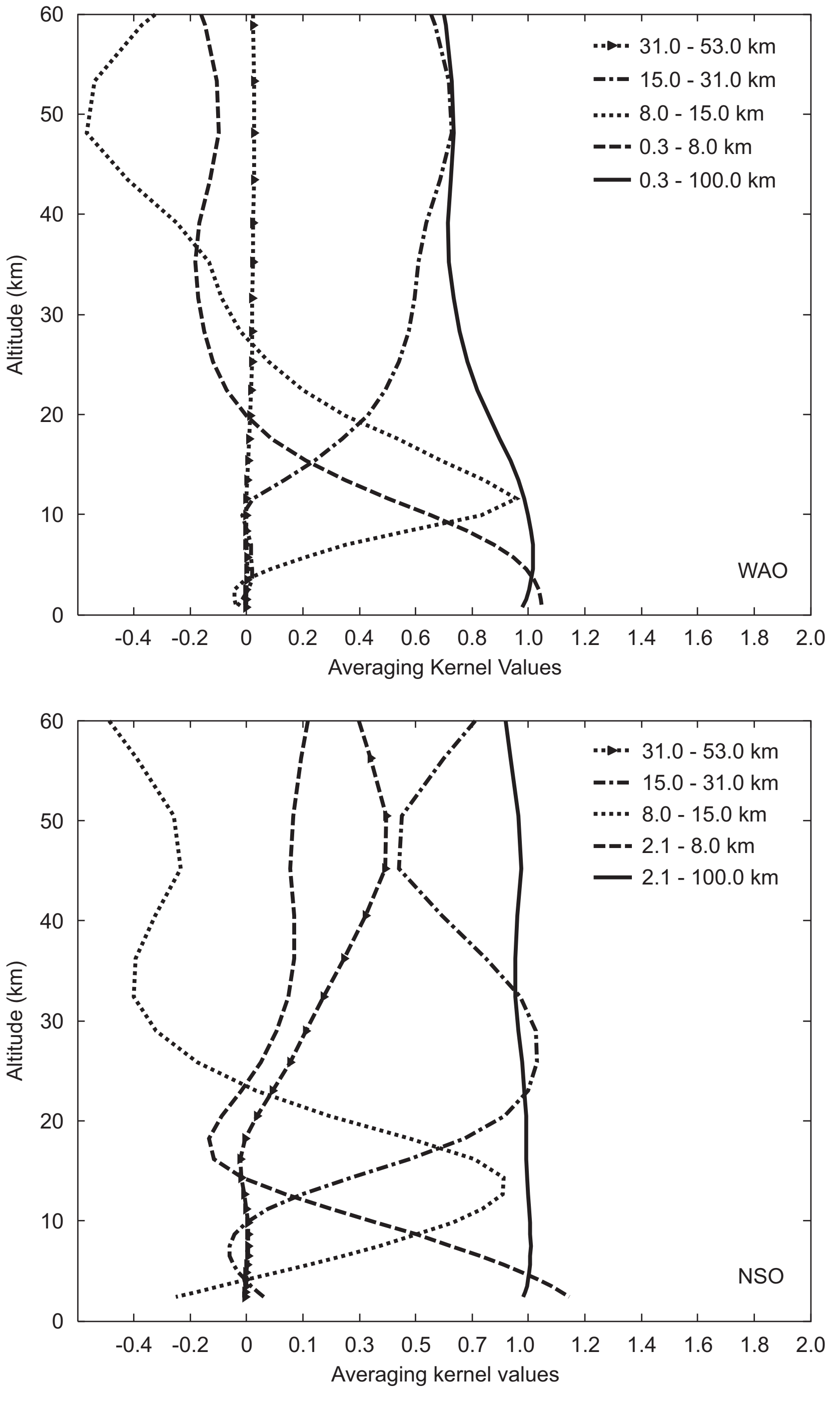

Fig. 14. Averaging kernel profiles for the retrievals using CO_2 6348 cm^{-1} band at 1.57 μm recorded at WAO on 22 November 2006 (spectral resolution: 0.1 cm^{-1}, solar zenith angle: 66.6°) and using spectra recorded at NSO on 25 July 2005 (spectral resolution: 0.01 cm^{-1}, solar zenith angle: 49.1°) are shown in the upper and lower plots, respectively.

The common systematic errors such as surface pressure, scattering effects of large particles in the solar beam are removed by using Eqs. (3) and (4). Fig. 16 shows the retrieved total column of CO_2 and O_2 together with the column-averaged VMR of CO_2 in dry air observed at the two sites. Fig. 17 presents the retrieved total column and column-averaged VMR in dry air of CH_4. The precision of the observations can be estimated

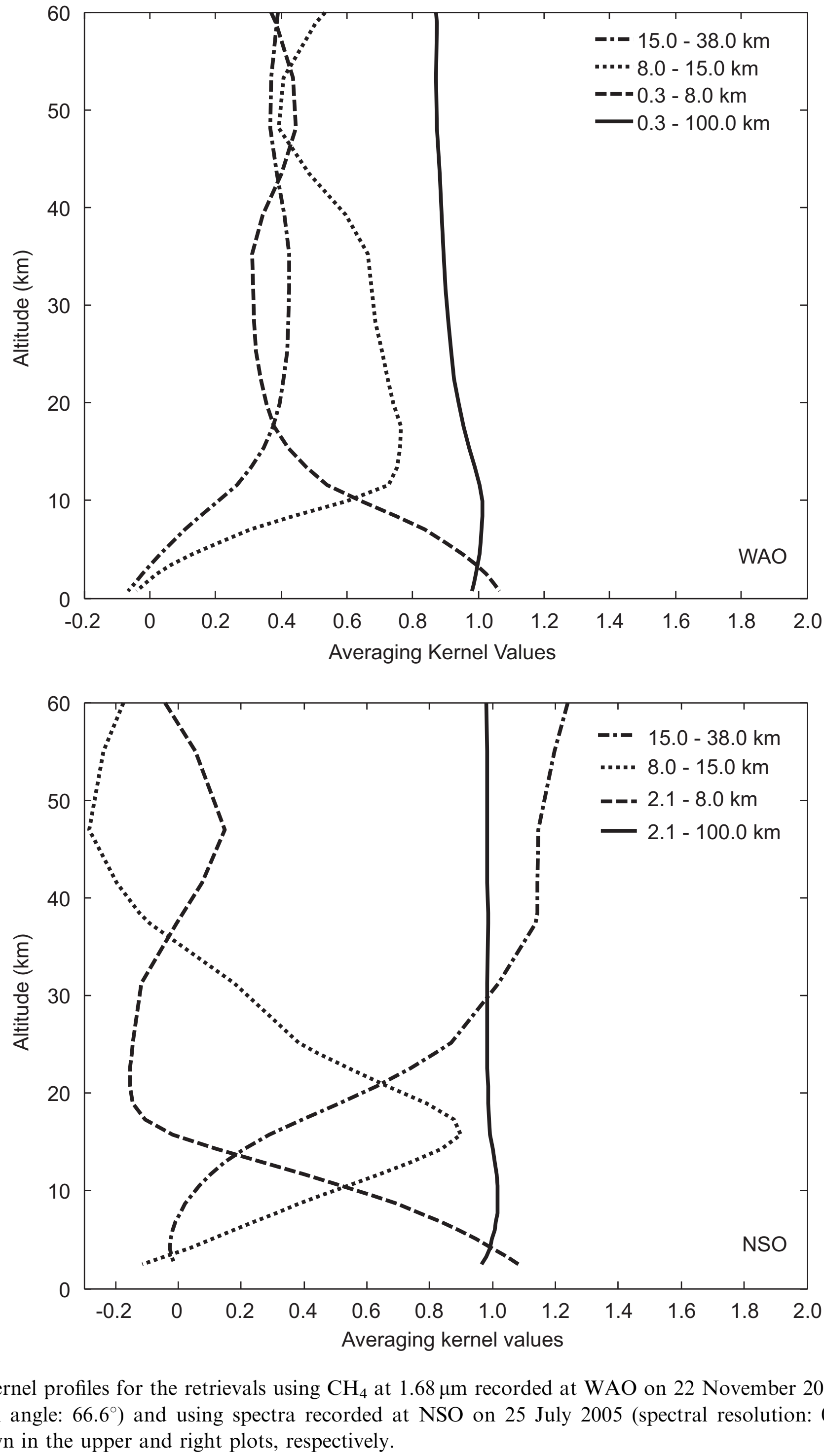

Fig. 15. Averaging kernel profiles for the retrievals using CH_4 at 1.68 μm recorded at WAO on 22 November 2006 (spectral resolution: $0.1\,cm^{-1}$, solar zenith angle: 66.6°) and using spectra recorded at NSO on 25 July 2005 (spectral resolution: $0.01\,cm^{-1}$, solar zenith angle: 49.1°) are shown in the upper and right plots, respectively.

from one sigma standard deviation of the results of repeated measurements under similar conditions. The measurements at each site were performed in a single day with uniform weather conditions. The precisions of the column-averaged VMRs of CO_2 and CH_4 in dry air are found to be better than 1.07% and 1.13%, respectively, computed as the standard deviation of the WAO data presented in Figs. 16 and 17.

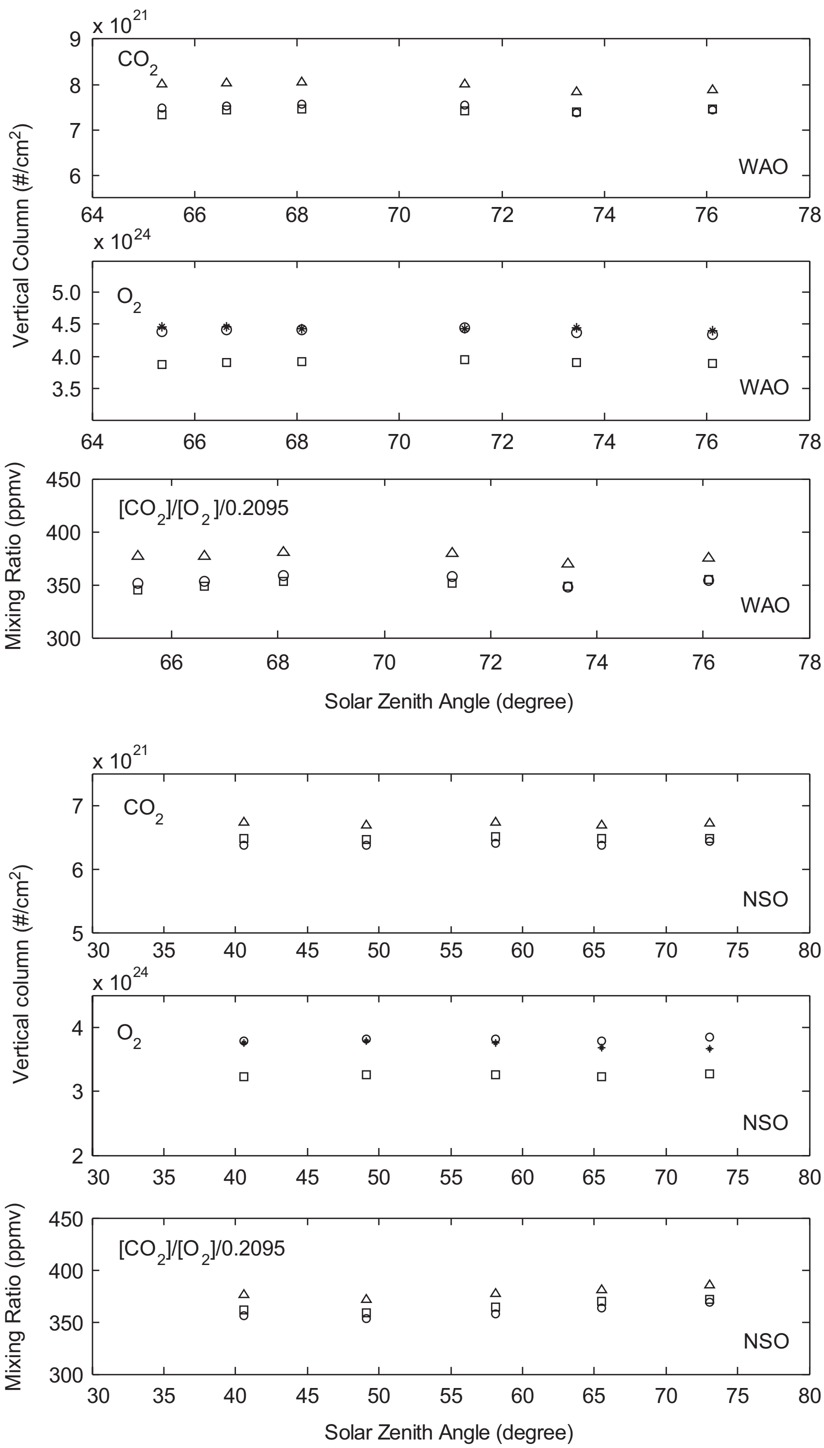

Fig. 16. Retrieved total vertical column densities of CO_2, O_2 and column ratios of CO_2 to O_2 obtained using spectra recorded at WAO on 22 November 2006 (spectral resolution: $0.1\,cm^{-1}$) and using spectra recorded at NSO on 25 July 2005 (spectral resolution: $0.01\,cm^{-1}$) are shown in the upper plot and lower plots, respectively, as a function of solar zenith angles. In both plots, top panels contain retrieved total columns of CO_2 at 1.57 and 2.06 μm (triangles: $6348\,cm^{-1}$ band at 1.57 μm; circles: $6228\,cm^{-1}$ band at 1.57 μm; squares: 2.06 μm band); middle panels present retrieved total columns of O_2 at 1.27 μm and at 0.76 μm (circles: 1.27 μm band with HITRAN 2004 spectroscopic parameters; squares: 1.27 μm band with Goldman spectroscopic parameters; stars: 0.76 μm band with HITRAN 2004 spectroscopic parameters); bottom panels show volume mixing ratios (VMR) of CO_2 in dry air at 1.57 and 2.06 μm corrected with simultaneously observed total columns of O_2 at 0.76 μm (triangles: $6348\,cm^{-1}$ band at 1.57 μm; circles: $6228\,cm^{-1}$ band at 1.57 μm; squares: 2.06 μm band).

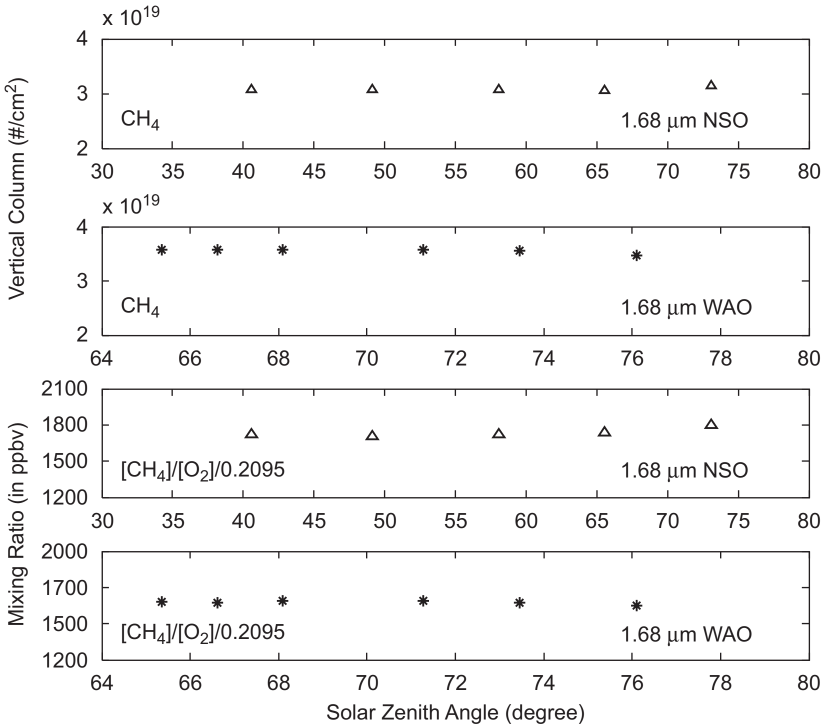

Fig. 17. Retrieved total columns of CH_4 at 1.68 μm from observations at NSO, retrieved total columns of CH_4 at 1.68 μm from observations at WAO, and volume mixing ratios (VMR) of CH_4 at 1.68 μm corrected with simultaneously observed total columns of O_2 at 0.76 μm at NSO, and VMRs of CH_4 in dry air at 1.68 μm corrected with simultaneously observed total columns of O_2 at 0.76 μm at WAO are shown in plots from the top to the bottom, respectively. Observations at WAO and NSO are on 22 November 2006 with a spectral resolution of 0.1 cm^{-1} and 25 July 2005 with a spectral resolution of 0.01 cm^{-1}, respectively.

The observed values for the precision of total column densities at WAO about 1% are in general agreement with other values in the literature. Yang et al. in 2002 [7] state that they obtain a precision better than 0.5% for CO_2 mixing ratios for most of observations made from 1978 to 1985 at the McMath–Pierce telescope complex on the Kitt Peak. However, this value is obtained by rejecting many of the observations, particularly those with an airmass greater than 2. Fig. 4 of Yang et al.'s paper shows that a precision of about 1% over a range of solar zenith angles is obtained, similar to our work. Washenfelder et al. in 2006 quote a precision about 0.1% for the average CO_2 mixing ratio in dry air for observations made at the Wisconsin Tall Tower site [42]. These observations were made in 1 h at solar noon as shown in Fig. 4 of Washenfelder et al.'s paper [42]. Taking the entire data set into account, the retrieved columns of CO_2 show a systematic trend of about 1%, particularly for measurements made in the afternoon. In our work, the precision was calculated using about 4 h of observations made in the afternoon. All of these observations have satisfactory SNRs and precisions to satisfy the requirements (i.e., about 0.3% or 1 ppm) for validation of space-based dry VMR measurements of greenhouse gases since the precision can be improved in various ways (e.g., limiting the range of solar zenith angles used, rejecting outliers, or accumulating a large number of observations).

The observed total columns of CO_2, CH_4, and O_2 at NSO in all of spectral regions are less than those in WAO about 12%, 15%, and 11%, respectively. These differences are reasonable because of the different altitudes of two observation sites (NSO: 2.1 km above sea level; WAO: 0.3 km). The column densities of CO_2 from the 6348 cm^{-1} band are consistently higher than those derived from the 6228 cm^{-1} band and 2.06 μm band by about 7%. The column densities of O_2 from the 0.76 μm band show differences of about 1.5% from those derived using the 1.27 μm band. Note that the 1.27 μm band cannot be used for normalization by CC-FTS because it would be heavily contaminated by airglow. The Goldman spectroscopic parameters for O_2 1.27 μm band provide O_2 amounts 12% lower than those obtained using the values in HITRAN 2004, although the fitting residuals are improved. The systematic residuals that are observed in our analysis are due to deficiencies in the line parameters.

Observations in nadir mode made from space are different from ground-based solar observations in terms of signal intensity and measurement modes, although the requirements on spectral resolution and sensitivity for vertical sampling are fairly similar. Hence, there are two primary observation modes for CC-FTS: nadir viewing and glint viewing for land and water surfaces, respectively. The glint viewing geometry uses the mirror-like specular reflection of sunlight from a flat water surface. The reason for using the glint viewing geometry is that in the short wave infrared bands (about 4000–6500 cm^{-1}), the albedo (the ratio of reflected to incident radiation) of water is too low, $<1\%$, to provide a suitable source of radiance. The glint viewing geometry provides a higher radiance similar to a typical nadir view over land. In nadir viewing geometry, the CC-FTS will scan from west to the east to obtain cross track observations and will have a total field of view (FOV) of 8 by 8 km. An 8 by 8 array of independent InGaAs or Si detectors placed in a square array will be used. Detector arrays are used to increase the overall throughput, to allow the rejection of cloud-covered pixels and to increase the SNR by co-adding the clear-view pixels. The SNR increases with the square root of the number of co-added pixels. Based on studies carried out by ABB-Bomem, in the nadir observation mode the SNR ranges from 160:1 to 600:1. A single scan of the FTS lasting 6.5 s yields a set of 64 interferograms for each FOV. Each detector pixel is identical and observes 1 km^2 within the 8 km^2. Motion compensation is also required using a tracker in order to keep the FOV constant for 6.5 s.

5. Summary and conclusions

Atmospheric spectra with resolutions of 0.0042, 0.01, 0.1, and 0.3 cm^{-1} in the 3950–7140 cm^{-1} region recorded at the Swedish Institute of Space Physics (IRF) in Kiruna, Sweden, are compared. The spectral features of CH_4, N_2O, CO, and CO_2 2.06 μm band are under-resolved in most spectral regions at a resolution of 0.3 cm^{-1}, which is similar to that used in the OCO mission. Spectra with a resolution of 0.1 cm^{-1} are sufficient to resolve the absorption features of CO_2, CH_4, N_2O, and CO.

In order to obtain the absorption features of CH_4, CO_2, CO, and N_2O together with the O_2 A-band in a single spectrum, further observations over a broad spectral region from 2000 to 15000 cm^{-1} were taken at Kitt Peak and Waterloo at a resolution of 0.01 and 0.1 cm^{-1}, respectively. The vertical sampling of these observations is quantified by computing averaging kernels as defined in the Rodgers optimal estimation method. The vertical sampling of observations with a spectral resolution of 0.1 cm^{-1} is similar to those with a spectral resolution of 0.01 cm^{-1}. A spectral resolution of 0.1 cm^{-1} (MOPD = 5 cm) is recommended for the CC-FTS mission.

Systematic fitting residuals are obvious in all of our retrievals and have been noted previously [7–9,41,42]. These residuals are due to the deficiencies in the spectroscopic line parameters in the HITRAN 2004 database. To improve the precision of atmospheric observations, new laboratory measurements on the spectroscopic parameters are required.

Acknowledgments

Funding for this work was provided by the Canada Space Agency (CSA) and the Natural Sciences and Engineering Research Council of Canada. We thank Dr. A. Meier and IRF for providing the atmospheric observation spectra recorded at Kiruna, Sweden. We are grateful for the spectroscopic parameters of O_2 1.27 μm band provided by A. Goldman.

References

[1] Etheridge DM, Steele LP, Francey RJ, Langenfelds RL. Atmospheric methane between 1000 A.D. and present: evidence of anthropogenic emissions and climate variability. J Geophys Res 1998;103(D13):15,979–93.

[2] Cunnold DM, Steele LP, Fraser PJ, Simmonds PG, Prinn RG, Weiss RF, et al. In situ measurements of atmospheric methane at GAGE/AGAGE sites during 1985–2000 and resulting source inferences. J Geophys Res 2002;107(D14):4225.

[3] Hofmann DJ, Butler JH, Dlugokencky EJ, Elkins JW, Masarie K, Montzka SA, et al. The role of carbon dioxide in climate forcing from 1979 to 2004: introduction of the annual greenhouse gas index. Tellus B 2006;58B:614–9.
[4] Intergovernmental Panel on Climate Change (IPCC). Climate change 2007: the physical science basis. Geneva, Switzerland: IPCC Secretariat; 2007.
[5] Keeling CD, Chin JFS, Whorf TP. Increased activity of northern vegetation inferred from atmospheric CO_2 measurements. Nature 1996;382:146–9.
[6] Keeling CD, Piper SC, Bacastow RB, Wahlen M, Whorf TP, Heimann M, et al. Atmospheric CO_2 and $^{13}CO_2$ exchange with the terrestrial biosphere and oceans from 1978 to 2000: observations and carbon cycle implications, in a history of atmospheric CO_2 and its effects on plants, animals, and ecosystems. In: Ehleringer JR, Cerling TE, Dearing MD, editors. New York: Springer; 2005.
[7] Yang Z, Toon GC, Margolis JS, Wennberg PO. Atmospheric CO_2 retrieved from ground-based near IR solar spectra. Geophys Res Lett 2002;29(9):1339.
[8] Washenfelder RA, Wennberg PO, Toon GC. Tropospheric methane retrieved from ground-based near-IR solar absorption spectra. Geophys Res Lett 2003;30(23):2226.
[9] Dufour E, Bréon F, Peylin P. CO_2 column averaged mixing ratio from inversion of ground-based solar spectra. J Geophys Res 2004;109:D09304.
[10] Keeling CD. The concentration and isotopic abundances of carbon dioxide in the atmosphere. Tellus 1960;12:200–3.
[11] Houghton JT, Ding Y, Griggs DJ, Noguer M, Linden PJ, Dai X, et al. Climate change 2001: the scientific basis. Cambridge: Cambridge University Press; 2000.
[12] Gurney KR, Law RM, Denning AS, Rayner PJ, Baker D, Bousquet P, et al. Towards robust regional estimates of CO_2 sources and sinks using atmospheric transport models. Nature 2002;415:626–30.
[13] Rayner PJ, O'Brien DM. The utility of remotely sensed CO_2 concentration data in surface source inversions. Geophys Res Lett 2001;28(1):175–8.
[14] O'Brien DM, Rayner PJ. Global observations of the carbon budget: 2. CO_2 column from differential absorption of reflected sunlight in the 1.61 μm band of CO_2. J Geophys Res 2002;107(D18):4354.
[15] Rayner PJ, Law RM, O'Brien DM, Butler TM, Dilley AC. Global observations of the carbon budget: 3. Initial assessment of the impact of satellite orbit, scan geometry, and cloud on measuring CO_2 from space. J Geophys Res 2002;107(D21):4557.
[16] Dufour E, Bréon F. Spaceborne estimate of atmospheric CO_2 column by use of the differential absorption method: error analysis. Appl Opt 2003;42(18):3595–609.
[17] Mao J, Kawa SR. Sensitivity studies for space-based measurement of atmospheric total column carbon dioxide by reflected sunlight. Appl Opt 2004;43:914–27.
[18] Miller CE, Crisp D, DeCola PL, Olsen SC, Randerson JT, Michalak AM, et al. Precision requirements for space-based X_{CO_2} data. J Geophys Res 2007;112:D10314.
[19] Chédin A, Hollingsworth A, Scott NA, Serrar S, Crevoisier C, Armante R. Annual and seasonal variations of atmospheric CO_2, N_2O and CO concentrations retrieved from NOAA/TOVS satellite observations. Geophys Res Lett 2002;29(8):1269.
[20] Chédin A, Saunders R, Hollingsworth A, Scott N, Matricardi M, Etcheto J, et al. The feasibility of monitoring CO_2 from high-resolution infrared sounders. J Geophys Res 2003;108(D2):4064.
[21] Aumann HH, Chahine MT, Gautier C, Goldberg MD, Kalnay E, McMillin LM, et al. AIRS/AMSU/HSB on the Aqua mission: design, science objectives, data products, and processing systems. IEEE Trans Geosci Remote Sensing 2003;41(2):253–64.
[22] Turquety S, Hadji-Lazaro J, Clerbaux C, Hauglustaine DA, Clough SA, Cassé V, et al. Operational trace gas retrieval algorithm for the infrared atmospheric sounding interferometer. J Geophys Res 2004;109:D21301.
[23] Beer R. TES on the Aura mission: scientific objectives, measurements, and analysis overview. IEEE Trans Geosci Remote Sensing 2006;44(5):1102–5.
[24] Drummond JR, Mand GS. The measurements of pollution in the troposphere (MOPITT) instrument: overall performance and calibration requirements. J Atmos Oceanic Technol 1996;13:314–20.
[25] Deeter MN, Emmons LK, Edwards DP, Gille JC, Drummond JR. Vertical resolution and information content of CO profiles retrieved by MOPITT. Geophys Res Lett 2004;31:L15112.
[26] Buchwitz M, Beek RD, Noël S, Burrows JP, Bovensmann H, Bremer H, et al. Carbon monoxide, methane and carbon dioxide columns retrieved from SCIAMACHY by WFM-DOAS: year 2003 initial data set. Atmos Chem Phys 2005;5:3313–29.
[27] Frankenberg C, Meirink JF, van Weele M, Platt U, Wagner T. Assessing methane emissions from global space-borne observations. Science 2005;308:1010–4.
[28] Crisp D, Atlas RM, Breon FM, Brown LR, Burrows JP, Ciais P, et al. The orbiting carbon observatory (OCO) mission. Adv Space Res 2004;34(4):700–9.
[29] Park JH. Atmospheric CO_2 monitoring from space. Appl Opt 1997;36(12):2701–12.
[30] Hamazaki T, Kaneko Y, Kuze A, Kondo K. Fourier transform spectrometer for greenhouse gases observing satellite (GOSAT). SPIE 2005;5659:73–80.
[31] Frankenberg C, Platt U, Wagner T. Iterative maximum a posteriori (IMAP)-DOAS for retrieval of strongly absorbing trace gases: model studies for CH_4 and CO_2 retrieval from near infrared spectra of SCIAMACHY onboard ENVISAT. Atmos Chem Phys 2005;5:9–22.
[32] Bösch H, Toon GC, Sen B, Washenfelder RA, Wennberg PO, Buchwitz M, et al. Space-based near-infrared CO_2 measurements: testing the Orbiting Carbon Observatory retrieval algorithm and validation concept using SCIAMACHY observations over Park Falls, Wisconsin. J Geophys Res 2006;111:D23302.

[33] Bovensmann H, Burrows JP, Buchwitz M, Frerick I, Noël S, Rozanov VV, et al. SCIAMACHY: mission objectives and measurement modes. J Atmos Sci 1999;56(2):127–50.
[34] Henningsen J, Simonsen H. The (2201–0000) band of CO_2 at 6348 cm^{-1}: linestrengths, broadening parameters, and pressure shifts. J Mol Spectrosc 2000;203(1):16–27.
[35] Miller CE, Brown LR. Near infrared spectroscopy of carbon dioxide I. $^{16}O^{12}C^{16}O$ line positions. J Mol Spectrosc 2004;228(2):329–54.
[36] Toth RA, Brown LR, Miller CE, Devi VM, Benner DC. Line strengths of $^{12}C^{16}O_2$: 4550–7000 cm^{-1}. J Mol Spectrosc 2006; 239(2):221–42.
[37] O'Brien DM, Mitchell RM, English SA, Da Costa GA. Airborne measurements of air mass from O_2 A-band absorption spectra. J Atmos Ocean Technol 1998;15:1272–86.
[38] Heidinger AK, Stephens GL. Molecular line absorption in a scattering atmosphere. Part II: application to remote sensing in the O_2 A-band. J Atmos Sci 2000;57:1615–34.
[39] Kuze A, Chance KV. Analysis of cloud-top height and cloud coverage from satellites using the O_2 A-band and B-bands. J Geophys Res 1994;99(D7):14,481–91.
[40] Asano S, Shiobara M, Uchiyama A. Estimation of cloud physical parameters from airborne solar spectral reflectance measurements for stratocumulus clouds. J Atmos Sci 1995;52(20):3,556–76.
[41] Yang Z, Wennberg PO, Cageao RP, Pongetti TJ, Toon GC, Sander SP. Ground-based photon path measurements from solar absorption spectra of the O_2 A-band. JQSRT 2005;90(3–4):309–21.
[42] Washenfelder RA, Toon GC, Blavier JF, Yang Z, Allen NT, Wennberg PO, et al. Carbon dioxide column abundances at the Wisconsin tall tower site. J Geophys Res 2006;111:D22305.
[43] Meier A, Toon GC, Rinsland CP, Goldman A, Hase F. Spectroscopic atlas of atmospheric microwindows in the middle infra-red, second edition. IRF technical report no.48, ISSN 0284-1738, Kiruna, April 2004.
[44] Pougatchev NS, Connor BJ, Rinsland CP. Infrared measurements of the ozone vertical distribution above Kitt Peak. J Geophys Res 1995;100(D8):16,689–97.
[45] Rinsland CP, Jones NB, Connor BJ, Logan JA, Pougatchev NS, Goldman A, et al. Northern and southern hemisphere ground-based infrared spectroscopic measurements of tropospheric carbon monoxide and ethane. J Geophy Res 1998;103(D21):28,197–217.
[46] Rodgers CD. Retrieval of atmospheric temperature and composition from remote measurements of thermal radiation. Rev Geophys Space Phys 1976;14(4):609–24.
[47] Rodgers CD. Characterization and error analysis of profiles retrieved from remote sounding measurements. J Geophys Res 1990; 95(D5):5587–95.
[48] Rodgers CD. Inverse methods for atmospheric sounding: theory and practice. Singapore: World Scientific; 2000.
[49] Rodgers CD, Connor BJ. Intercomparison of remote sounding instruments. J Geophys Res 2003;108(D3):4116.
[50] Meier A, Goldman A, Manning PS, Stephen TM, Rinsland CP, Jones NB, et al. Improvements to air mass calculations for ground-based infrared measurements. JQSRT 2004;83(1):109–13.
[51] Wiacek A, Taylor JR, Strong K, Saari R, Kerzenmacher TE, Jones NB, et al. Ground-based solar absorption FTIR spectroscopy: a novel optical design instrument at a new NDSC complementary station, characterization of retrievals and first results. J. Atmos Ocean Technol 2007;24(3):432–8.
[52] Wiacek A. First trace gas measurements using Fourier transform infrared solar absorption spectroscopy at the University of Toronto Atmospheric Observatory. PhD thesis, University of Toronto, 2006.
[53] Russell JM, Gordley LL, Deaver LE, Thompson RE, Park JH. An overview of the Halogen Occultation Experiment (HALOE) and preliminary results. Adv Space Res 1994;14(9):13–20.
[54] Carli B, Alpaslan D, Carlotti M, Castelli E, Ceccherini S, Dinelli BM, et al. First results of MIPAS/ENVISAT with operational Level 2 code. Adv Space Res 2004;33(7):1,012–9.
[55] Peterson DB, Margitan JM. Upper Atmospheric Research Satellite. Correlative Measurements Program (UARS-CMP) balloon data atlas. Washington, DC: NASA; 1995.
[56] SPARC. SPARC assessment of upper tropospheric and stratospheric water vapour, stratospheric processes and their role in climate. WCRP-113, WMO-TD No. 1043, SPARC report 2. Verrieres Le Buisson Cedex, 2000. p. 312.
[57] Bernath PF, McElroy CT, Abrams MC, Boone CD, Butler M, Camy-Peyret C, et al. Atmospheric chemistry experiment (ACE): mission overview. Geophys Res Lett 2005;32:L15S01.
[58] Boone CD, Nassar R, Walker KA, Rochon Y, McLeod SD, Rinsland CP, et al. Retrievals for the atmospheric chemistry experiment Fourier transform spectrometer. Appl Opt 2005;44(33):7218–31.
[59] McPherson RD, Bergan KH, Kistler RE, Rasch GE, Gordon DS. The NMC operational global data assimilation system. Mon Weather Rev 1979;107(11):1445–61.
[60] Kalnay E, Kanamitsu M, Kistler R, Collins W, Deaven D, Gandin L, et al. The NCEP/NCAR 40-year reanalysis project. Bull Am Meteorol Soc 1996;77(3):437–71.
[61] Picone JM, Hedin AE, Drob DP, Aikin AC. NRLMSISE-00 empirical model of the atmosphere: statistical comparison and scientific issues. J Geophys Res 2002;107(A12):1468–83.
[62] Rothman LS, Jacquemart D, Barbe A, Benner DC, Birk M, Brown LR, et al. The HITRAN 2004 molecular spectroscopic database. JQSRT 2005;96:139–204.
[63] Kuang Z, Margolis J, Toon G, Crisp D, Yung Y. Spaceborne measurements of atmospheric CO_2 by high-resolution NIR spectrometry of reflected sunlight: an introductory study. Geophys Res Lett 2002;29(15):1716.
[64] Devi VM, Benner DC, Brown LR, Miller CE, Toth RA. Line mixing and speed dependence in CO_2 at 6348 cm^{-1}: positions, intensities and air- and self-broadening derived with constrained multispectrum analysis. J Mol Spectrosc 2007;242(2):90–117.

[65] Miller CE, Montgomery MA, Onorato RM, Johnstone C, McNicholas TP, Kovaric B, et al. Near infrared spectroscopy of carbon dioxide. II: $^{16}O^{13}C^{16}O$ and $^{16}O^{13}C^{18}O$ line positions. J Mol Spectrosc 2004;228(2):355–74.
[66] Miller CE, Brown LR, Toth RA, Benner DC, Devi VM. Spectroscopic challenges for high accuracy retrievals of atmospheric CO_2 and the Orbiting Carbon Observatory (OCO) experiment. C R Phys 2005;6(8):876–87.
[67] Toth RA, Brown LR, Miller CE, Devi VM, Benner DC. Self-broadened widths and shifts of $^{12}C^{16}O_2$: 4750–7000 cm^{-1}. J Mol Spectrosc 2006;239(2):243–71.
[68] Boone CB, Walker KA, Bernath PF. Speed-dependent Voigt profile for water vapor in infrared remote sensing applications. JQSRT 2007;105:525–32.
[69] Barkley MP, Monks PS, Hewitt AJ, Machida T, Desai A, Vinnichenko N, et al. Assessing the near surface sensitivity of SCIAMACHY atmospheric CO_2 retrieved using (FSI) WFM-DOAS. Atmos Chem Phys 2007;7:3597–619.